Bioactive Materials 40 (2024) 280–305

Contents lists available at ScienceDirect

Bioactive Materials

journal homepage: www.keaipublishing.com/en/journals/bioactive-materials

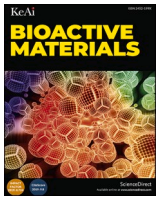

Review article

Liver tissue engineering using decellularized scaffolds: Current progress, challenges, and opportunities

Kamal H. Hussein [a,b,c], Boyukkhanim Ahmadzada [a,b], Julio Cisneros Correa [a,b], Ahmer Sultan [a,b], Silvana Wilken [a,b], Bruce Amiot [a,b], Scott L. Nyberg [a,b,*]

[a] Department of Surgery, Mayo Clinic, Rochester, MN, United States
[b] William J. von Liebig Center for Transplantation and Clinical Regeneration, Mayo Clinic, Rochester, MN, United States
[c] Department of Surgery, Anesthesiology, and Radiology, College of Veterinary Medicine, Assiut University, Assiut, Egypt

ARTICLE INFO

Keywords:
Bioengineered liver
Decellularization
Recellularization
Reendothelialization
Biliary reconstruction

ABSTRACT

Liver transplantation represents the only definitive treatment for patients with end-stage liver disease. However, the shortage of liver donors provokes a dramatic gap between available grafts and patients on the waiting list. Whole liver bioengineering, an emerging field of tissue engineering, holds great potential to overcome this gap. This approach involves two main steps; the first is liver decellularization and the second is recellularization. Liver decellularization aims to remove cellular and nuclear materials from the organ, leaving behind extracellular matrices containing different structural proteins and growth factors while retaining both the vascular and biliary networks. Recellularization involves repopulating the decellularized liver with appropriate cells, theoretically from the recipient patient, to reconstruct the parenchyma, vascular tree, and biliary network. The aim of this review is to identify the major advances in decellularization and recellularization strategies and investigate obstacles for the clinical application of bioengineered liver, including immunogenicity of the designed liver extracellular matrices, the need for standardization of scaffold fabrication techniques, selection of suitable cell sources for parenchymal repopulation, vascular, and biliary tree reconstruction. *In vivo* transplantation models are also summarized for evaluating the functionality of bioengineered livers. Finally, the regulatory measures and future directions for confirming the safety and efficacy of bioengineered liver are also discussed. Addressing these challenges in whole liver bioengineering may offer new solutions to meet the demand for liver transplantation and improve patient outcomes.

1. Introduction

Chronic liver diseases including cirrhosis, viral hepatitis, and hepatic cancer remain among the main causes of mortality worldwide, with approximately two million deaths annually, representing 4 % of all deaths worldwide [1]. Additionally, liver diseases are associated with a high economic and financial burden attributed to the cost of health care utilization. For instance, the expenditure of USA health care for patients with liver diseases exceeded $32.5 billion in 2016 [2]. Allogenic liver transplantation is still the gold standard curative option, especially for patients suffering from end-stage liver disease. Despite liver transplantation being the second most common solid organ transplantation worldwide, a notable gap persists between the number of available liver donors and patients on the waiting list [3]. This gap has resulted in less than 10 % of the global need for liver transplantation being fulfilled, leading to a marked rise in mortality among patients on the waiting list [1].

To close this gap, researchers investigated different alternative therapeutic strategies using tissue engineering approaches. Tissue engineering, as a preeminent area of regenerative medicine, aims to combine scaffolds, cells, and biologically active molecules into functional tissues that can restore, maintain, or improve damaged tissues or whole organs [4]. Decellularization, as a tissue engineering technique, has been used to provide an available pool of organs for future

Peer review under responsibility of KeAi Communications Co., Ltd.
* Corresponding author. Liver Regenerative Medicine, Artificial Liver Program, 200 First Street SW, Rochester, MN 55905, United States.
E-mail addresses: Youssif.Kamaleldin@mayo.edu (K.H. Hussein), Ahmadzada.Boyukhanim@mayo.edu (B. Ahmadzada), CesarCisnerosCorrea.Julio@mayo.edu (J.C. Correa), Sultan.Ahmer@mayo.edu (A. Sultan), Wilken.Silvana@mayo.edu (S. Wilken), Amiot.Bruce@mayo.edu (B. Amiot), Nyberg.Scott@mayo.edu (S.L. Nyberg).

https://doi.org/10.1016/j.bioactmat.2024.06.001
Received 3 April 2024; Received in revised form 30 May 2024; Accepted 1 June 2024

transplantation (Fig. 1). Decellularization has been defined as the maximal removal of cellular and nuclear material from a tissue or organ while preserving the biochemical composition, biological activity, three-dimensional organization, and integrity of the extracellular matrix using chemical, physical, and/or biological methods [5,6]. If successful, decellularization would result in developing scaffolds that mimic the mechanical, biological, and anatomical properties of native tissue [7]. After decellularization, the liver scaffold requires seeding with new cells that exhibit appropriate characteristics and functions. In addition to liver parenchymal cells, the reconstruction of the blood vessel and biliary tree network is necessary to produce a fully functional bioengineered liver that can potentially be transplanted into humans.

Several published studies have demonstrated promising results in generating bioengineered livers [8–14]. In this review, recent progress in bioengineered liver fabrication is explored, with a focus on significant obstacles such as extracellular matrix immunogenicity, the standardization of decellularization techniques, and the identification of suitable cell types for recellularization, reendothelialization, and biliary tree reconstruction. Furthermore, a summary of different *in vivo* transplantation models utilized to assess the functionality of bioengineered livers is provided. Lastly, the review discusses regulatory measures and offers future perspectives for confirming the safety and efficacy of bioengineered liver therapies.

2. Sources of liver for decellularization

There are various sources of liver for potential decellularization. Over the last two decades, livers from mice, rats, ferrets, rabbits, sheep, pigs, and humans have been used for decellularization [8–11,13–27]. From a clinical perspective, decellularized livers from mice, rats, ferrets, and rabbits are not suitable for human clinical transplantation due to their small liver size and other physiological differences. Livers that are unsuitable for allogenic human transplantation due to prolonged ischemia, excessive steatosis, size mismatch, or poor quality, may serve as a favorable source. In 2016, 739 livers were procured but not transplanted, representing 9 % of total transplants in USA [28]. By 2021, the number of the discarded livers had increased to 10 % of total transplants [29]. These discarded livers could potentially be used in the future for decellularization and recellularization processes.

One significant disadvantage of using human organs is the age-related changes of the extracellular matrix (ECM) [30–32]. It has been reported that with increasing age, the stiffness of the liver increases and elasticity decreases. This is attributed to an increase in collagen content, scar tissue formation, and cross-linking of the ECM caused by the accumulation of advanced glycation end-products on the ECM [33,34]. These changes in ECM microstructure can increase resistance to enzymatic digestion of the ECM and lead to significant discrepancies between human livers [30,31,35–38].

Pigs are considered the most suitable source for human-scale liver bioengineering owing to the organ size matching, availability, rapid maturation, production of large litters, similarity of the physiological metabolism and immune system with those of human, and the significant progress in genetic engineering techniques in pigs over the last decade [39,40]. The ease of obtaining pig livers of similar age may limit the impact of age-related biological differences in the ECM, thereby facilitating the standardization of decellularization processes. Therefore, liver harvested from pathogen-free pigs could be an important source for bioengineering livers for transplantation purposes.

3. Differences between porcine and human liver

Since porcine livers could be a potential source for transplantation, detailed knowledge of the differences between the porcine and human liver in terms of structure and microstructure is necessary. The average adult human liver is a wedge-shaped organ divided into 2 lobes (right and left), with a mean volume of 1862 cm^3. In contrast, the porcine adult liver is lobular clover leaf-shaped and divided into 4 lobes (right lateral, right median, left median, and left lateral lobes) with a mean volume of 652–1120 cm^3. Despite these differences, both livers are divided into 8 similar segments, as determined by previous studies [41–43].

The hepatic artery in the human liver has two branches, the left and right hepatic artery, which supply the corresponding lobe of the liver [44]. In pigs, the hepatic artery divides into right and left branches before reaching the hilum. The right branch further bifurcates into two branches, namely the ramus dexter medialis and the ramus dexter lateralis, providing vascular supply to the right lobe of the liver. Similarly, the left branch also divides into 3 main arteries, the ramus sinister medialis and ramus sinister lateralis (both supply the left lobe), and the ramus quadratus, which supplies the quadrate lobe and gallbladder [45,46]. Based on these findings, it can be concluded that no significant difference was recorded in the arterial blood supply between pigs and the human liver.

The portal veins of human and porcine liver exhibit a few differences. In pigs, the portal vein divides into right and left branches at the hilum, while in humans, this division occurs before entering the liver parenchyma. Additionally, there are communicating branches between the right median and right lateral rami of the portal vein. These branches traverse the fissure between the right lateral and right median lobes of the liver [47].

In humans, the venous drainage of the liver occurs through three

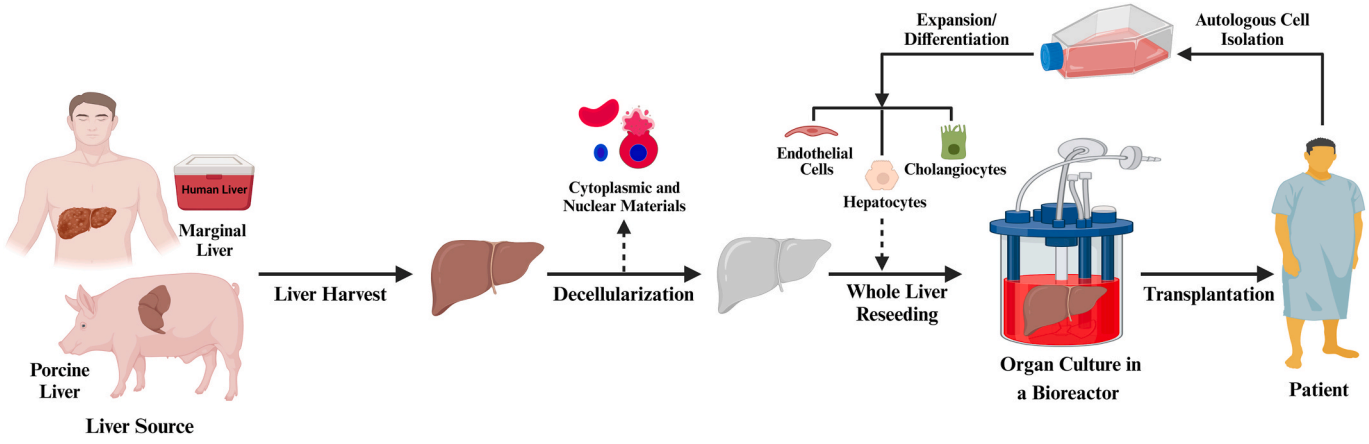

Fig. 1. Schematic overview of the development of a bioengineered liver from decellularized matrices. Marginal human livers, unsuitable for transplantation, and porcine livers are decellularized and subsequently recellularized with various cell types isolated from the patient. These cells are then cultured in a bioreactor to create a bioengineered liver that holds potential for transplantation into the patient.

hepatic veins (right, left, and middle). The middle hepatic vein shares the drainage of segment IV with the left hepatic vein and the drainage of segments V and VIII with the right hepatic vein [48]. In pigs, the liver drainage is accomplished by four thin veins that may be easily damaged during a surgical procedure. These veins drain the whole liver except Segment I which drains directly into the inferior vena cava. Importantly, the inferior vena cava passes through the liver parenchyma, which increases the difficulty in partial hepatectomy operations [47].

The biliary trees of both species are anatomically and functionally similar whereas the biliary ducts segmentation is identical to the portal vein segmentation due to their common track within the Glissonian sheath [49]. A distinctive feature of the biliary drainage of the pig liver is that the drainage of segment I is accomplished through the right hepatic duct in pigs, while in humans, it is drained through left hepatic duct [47].

In terms of the tissue microstructure, both porcine and human liver exhibits similarities. The parenchymal architecture is organized into well-defined, hexagonal lobules centered around the central vein with portal triads at its corners. These lobules consist of large polygonal hepatocytes stacked on top of each other and demarcated by fibrous septa containing variable amounts of connective tissue. These hepatocytes are estimated to be approximately 80 % of the liver tissue, while other non-parenchymal cells represent 20 % [50,51]. The portal triad consists of hepatic artery, portal vein, and bile duct and surrounded by loose connective tissue. Importantly, the hepatic sinusoids are located between the strips of hepatocytes, draining into the central vein [52]. The main histological difference is the presence of higher amount of collagen, especially in connective tissue septa that surround the lobules in pigs while these septa are absent in human liver parenchyma [53]. Estermann et al. evaluated the mechanical properties of both porcine and human liver [54]. They reported that porcine liver is stiffer than human liver, which may be attributed to the histological differences between the two tissues [53,54]. Additionally, porcine liver exhibited higher tensile loading compared to human liver, while no difference in the viscoelastic properties was reported [54,55].

4. Obstacles and challenges for clinical application of bioengineered liver

4.1. ECM immunogenicity

Organ decellularization, a key process in manufacturing ECM scaffolds, aims to eliminate immunogenic cellular materials, thus reducing the immunogenicity of allogenic and xenogeneic derived scaffolds [56]. Following implantation, these natural ECM scaffolds undergo a degree of degradation, releasing matricryptic peptides and growth factors. This process triggers a shift in macrophage polarization from pro-inflammatory (M1) phenotype to an anti-inflammatory regenerative phenotype (M2 macrophages), promoting angiogenesis and recruiting stem/progenitor cell toward the implanted tissue for constructive remodeling [5,57,58]. Overall, decellularized tissues may experience a lower rejection rate if they are completely depleted of the different sources of immunogens [7,59]. Factors such as the presence of DNA and xenogeneic epitopes, such as alpha-Gal and Neu5GC, as well as the age and integrity of the ECM, play important roles in influencing the immunogenicity of decellularized tissues.

4.1.1. DNA

Several researchers have emphasized the importance of residual DNA within scaffolds derived from porcine sources and its implications for immune responses post-implantation [60–62]. Although the specific threshold of residual DNA within the ECM sufficient to trigger a negative remodeling response has not been extensively studied, many researchers suggested that decellularized tissues should ideally have less than 50 ng dsDNA per mg ECM dry weight [5,7]. Recently, Record Ritchie et al. purified DNA from unprocessed porcine small intestine ECM and decellularized ECM before and after sterilization. They injected 50 μg of DNA into mice, with or without strong co-stimulators such as incomplete Freund's adjuvant, methylated bovine serum albumin, and interleukin-12 [63]. It is significant to mention that DNA isolated from unprocessed, aseptic, or sterilized porcine ECM, when injected without adjuvants, did not provoke a rejection response. Instead, it induced a mild accommodation cytokine response locally, with no systemic anti-DNA antibody expression observed, even at doses approximately 100-fold greater than those anticipated through ECM implantation. This study, combined with the fact that the Food and Drug Administration (FDA) does not impose limitations or restrictions on the presence of DNA in biological scaffolds, emphasizes that DNA content is not a reliable indicator of decellularization efficiency. The FDA's stance is based on product safety data submitted by manufacturers, which supports the view that DNA presence does not necessarily correlate with antigenicity. Consequently, it necessitates the exploration of an alternative and more precise criterion for evaluating the antigenicity of decellularized tissues.

4.1.2. Xeno-epitopes

Alpha-Gal epitopes (Galα1-3Galβ1-4GlcNAc-R) are specific carbohydrate structures found on the cell surface of non-primate mammals, such as pigs. These epitopes are absent in humans and Old-World monkeys due to mutations in the α1,3-galactosyl-transferase gene [64,65]. The absence of alpha-Gal epitopes in humans leads to the production of anti-Gal antibodies (approximately represent 1 % of serum antibodies), primarily due to exposure to intestinal bacteria carrying these epitopes [66]. The extensive presence of alpha-Gal in porcine tissues and organs, including liver, renders them vulnerable to rejection due to xenograft-specific immune responses. Decellularization has demonstrated efficient capability in removing or reducing the alpha-gal content from porcine liver [67–69].

Neu5Gc (N-Glycolylneuraminic acid) epitopes, in non-human mammals, is another significant antigen in rejection of xenografts. Humans lack functional cytidine monophospho-N-acetylneuraminic acid hydroxylase (CMAH), the enzyme responsible for converting Neu5Ac (N-acetylneuraminic acid) to Neu5GC, due to a genetic mutation, resulting in the absence of Neu5GC in human tissues [70,71]. Consequently, antibodies against Neu5GC, may be produced by humans, leading to hyperacute rejection of the graft containing this antigen [72]. Unfortunately, the presence of Neu5Gc antigen was not previously assessed during decellularization of porcine liver. Thus, the efficacy of depleting this antigen from the porcine liver remains uncertain, emphasizing the importance of further investigations to determine if specific enzymatic treatment after decellularization is required.

4.1.3. ECM alteration

ECM contains different cryptic peptides that can either stimulate or inhibit the host immune response [73]. Decellularization process may increase the immunogenicity of the tissue by exposing hidden immunogenic domains, converting inert molecules within the decellularized tissue into immunogenic particles, or depleting immunomodulatory substances [74]. For instance, harsh decellularization procedures may unveil certain cryptic helical and terminal antigenic sites of collagen, prompting the initiation of antibody production against the ECM [73]. Additionally, Adair-Kirk et al. showed that enzymatic treatment could lead to the release of a specific cryptic epitope of laminin α5, resulting in the liberation of a 16-amino acid peptide [75]. This peptide exhibited the ability to attract polymorphonuclear leukocytes (PMNs) and macrophages, as well as induce the production of matrix metalloproteinase-9 (MMP-9) from immune cells.

Damage to elastin can lead to the release of elastin peptides, either through harsh decellularization processes or the depletion of glycosaminoglycans (GAGs). GAGs play a crucial role in protecting elastin from protease activity [76–78]. The liberated elastin particles could induce monocyte chemotaxis, promote T helper cell differentiation into inflammatory phenotypes (TH1 and TH17), and contribute to

antibody-mediated inflammatory responses [79].

Moreover, high molecular weight hyaluronic acids, recognized GAGs within the decellularized ECM, exhibit anti-inflammatory effects by hindering the interaction between antigens and antibodies. They also activate toll-like receptors (TLRs), a specific subset of pattern recognition receptors (PRRs), as well as CD44 receptors found on innate and adaptive immune cells [80]. Activation of these receptors is associated with reduced dendritic cell maturation, enhanced macrophage polarization towards the M2 phenotype, T cell differentiation into a regulatory phenotype, and induction of apoptosis in activated T cells [80,81]. Conversely, low molecular weight hyaluronic acids are released when ECM undergoes damage or degradation. They enhance immune cell chemotaxis, dendritic cell maturation, and macrophage polarization toward the M1 phenotype, mediated through the same receptors, CD44 and TLRs [74].

4.1.4. Age of ECM

The age of the ECM source emerges as a crucial determinant influencing the immunological traits of ECM-based biomaterials. For instance, LoPresti and Brown investigated the influence of age using decellularized small intestine submucosa (SIS) derived from pigs of different ages (12, 26, and 52 weeks) on the phenotype and function of bone marrow macrophages obtained from mice aged 2 or 18 months [82]. According to the findings, SIS obtained from 52-week-old pigs elicited diminished iNOS production in 2-month macrophages and suppressed Fizz 1 expression in both 2 and 18-month macrophages in comparison to 12-week SIS. The study suggested that ECM derived from aged animals results in a distinct macrophage phenotype compared to younger controls, emphasizing the importance of sourcing ECM from young donors to maintain favorable outcomes in constructive remodeling of ECM biomaterials.

Importantly, myocardium harvested from older human cadaver hearts underwent additional lipid and DNA/RNA removal steps to remove greater adipose tissue commonly found on older human myocardium and reduce nucleotide content to similar acceptable standards for therapeutic applications as the porcine myocardial matrix, achieving fully decellularization of the tissue [83]. Moreover, the content of laminin, elastin, and growth factors decreases with age [30,37,84,85]. Therefore, considering the age of the tissue source is critical to expect the potential host immune response. Further research is required to investigate the optimal age for obtaining liver tissue for decellularization to produce decellularized scaffolds with a high content of growth factors and essential components necessary to facilitate recellularization and revascularization, achieving constructive remodeling *in vivo* before biodegradation.

4.2. Standardization of liver scaffold fabrication

4.2.1. Decellularization

Although the first attempts to isolate the extracellular matrix (ECM) from tissues were reported in the 1970s and 1980s [86–88], the first successful trial to decellularize a whole organ was achieved by Ott et al. in 2008 [89]. They successfully constructed a whole rat heart scaffold by perfusing detergents through the coronary artery for 12 h. This achievement marked a significant breakthrough in the field of whole organ tissue engineering. In 2010, Uygun et al. demonstrated the feasibility of obtaining a whole decellularized scaffold through the perfusion of the rat liver with detergent for 72 h [12]. After recellularization with rat hepatocytes, they transplanted the recellularized liver heterotopically for 8 h. Examination of the graft revealed the hepatocytes' ability to retain their normal morphology and function. Since then, several research groups have reported the liver decellularization using different methods and reagents [11,13,14,23].

4.2.1.1. Decellularization agents. Although various methods, including physical, chemical, and enzymatic treatments or a combination of them, have been used for liver decellularization (Fig. 2) [7], it is very difficult to consider one of those agents as an ideal method that efficiently balances the depletion of the cytoplasmic and nuclear content of the tissue and the preservation of essential structural and bioactive ECM components that can promote the attachment, growth, and differentiation of the reseeded cells.

4.2.1.1.1. Chemical methods. Chemical treatments, including ionic, non-ionic, and Zwitter-ionic detergents, alcohols, acids, alkalis, and hypotonic/hypertonic solutions, are commonly used for liver decellularization [5,12,21]. Although chemical agents play a key role in the decellularization and removal of the immunogenic materials from the decellularized tissues, they may cause ECM damage and affect the biocompatibility of the yielded decellularized tissues [5,7,90–92].

4.2.1.1.1.1. Detergents

Sodium dodecyl sulfate (SDS) and Triton X-100 are commonly used ionic and non-ionic agents, respectively for decellularization. SDS can denature proteins and lyse cells by disrupting protein-protein interactions, while Triton X-100 can disrupt lipid–lipid, lipid–protein, and DNA-protein interactions while preserving protein-protein interaction [7,59]. Subsequently, SDS is likely to negatively affect the ECM architecture and disrupt the structure of protein constituents, including collagens, whereas Triton X-100 exerts its effect on cells without altering the ECM protein structures [80,93]. Of note, research has shown that SDS-treated ECM scaffolds generally have higher reactivities upon implantation due to the disruption of collagen fiber structures and exposure of cryptic antigens [7,59,94]. However, one study reported that Triton X-100 tends to break DNA into larger fragments, which might induce an adverse tissue remodeling response. This finding indicates that while Triton X-100 preserves ECM protein structures better than SDS, it may still pose some immunogenic risks due to remnant DNA [95].

The effect of both SDS and Triton X-100 depends mainly on their concentrations; however, higher concentrations will cause detrimental effects on ECM components. Additionally, several studies have reported the cytotoxic effect of SDS and Triton X-100 on different cells, thus the use of lower concentrations and applying different washing cycles are required to yield scaffolds with minimal amounts of these chemicals [5,96,97]. Yielded decellularized scaffolds after terminal washing should contain less than 0.15 mM of Triton X-100; this concentration was shown to be tolerated by human cell lines [96]. Importantly, SDS concentrations beyond 10 μg/mg dry weight have shown cytotoxicity [98,99]. Several studies have reported the difficulty in completely washing out SDS from decellularized tissues via conventional washing methods due to the strong hydrophobic bonds between SDS and ECM proteins [68,100]. Washing decellularized scaffolds with CaCl2 could be applied to detoxify the remaining SDS via precipitation [92]. Interestingly, Triton X-100 could also be exploited to remove the residual SDS from decellularized tissues, suggesting SDS and Triton X-100 as an excellent combination for achieving almost complete cell removal, DNA removal, and minimization of cytotoxicity [95].

Ren et al. compared SDS and Triton X-100 for decellularization of the whole rat liver [101]. After perfusing the portal vein with SDS and Triton X-100, they observed a decrease in GAGs content to about 10 % and 50 %, elastin levels decreased to approximately 20 % and 60 %, and the amount of hepatocyte growth factor decreased to around 20 % and 60 % of the levels found in the native liver, respectively. This study indicated that Triton X-100 was much superior in preservation of the ECM than SDS. Furthermore, they reported that Triton X-100-treated scaffolds showed better liver-specific function, including albumin secretion, urea synthesis, ammonia elimination, and mRNA expression levels of drug metabolism enzymes upon reseeding with rat primary hepatocytes in a bioreactor for 7 days of culture compared to cells grown in SDS-treated scaffolds.

4.2.1.1.1.2. Acids and alkali

Acids and alkali can solubilize the cytoplasmic components of cells and remove nucleic materials by catalyzing the hydrolytic degradation

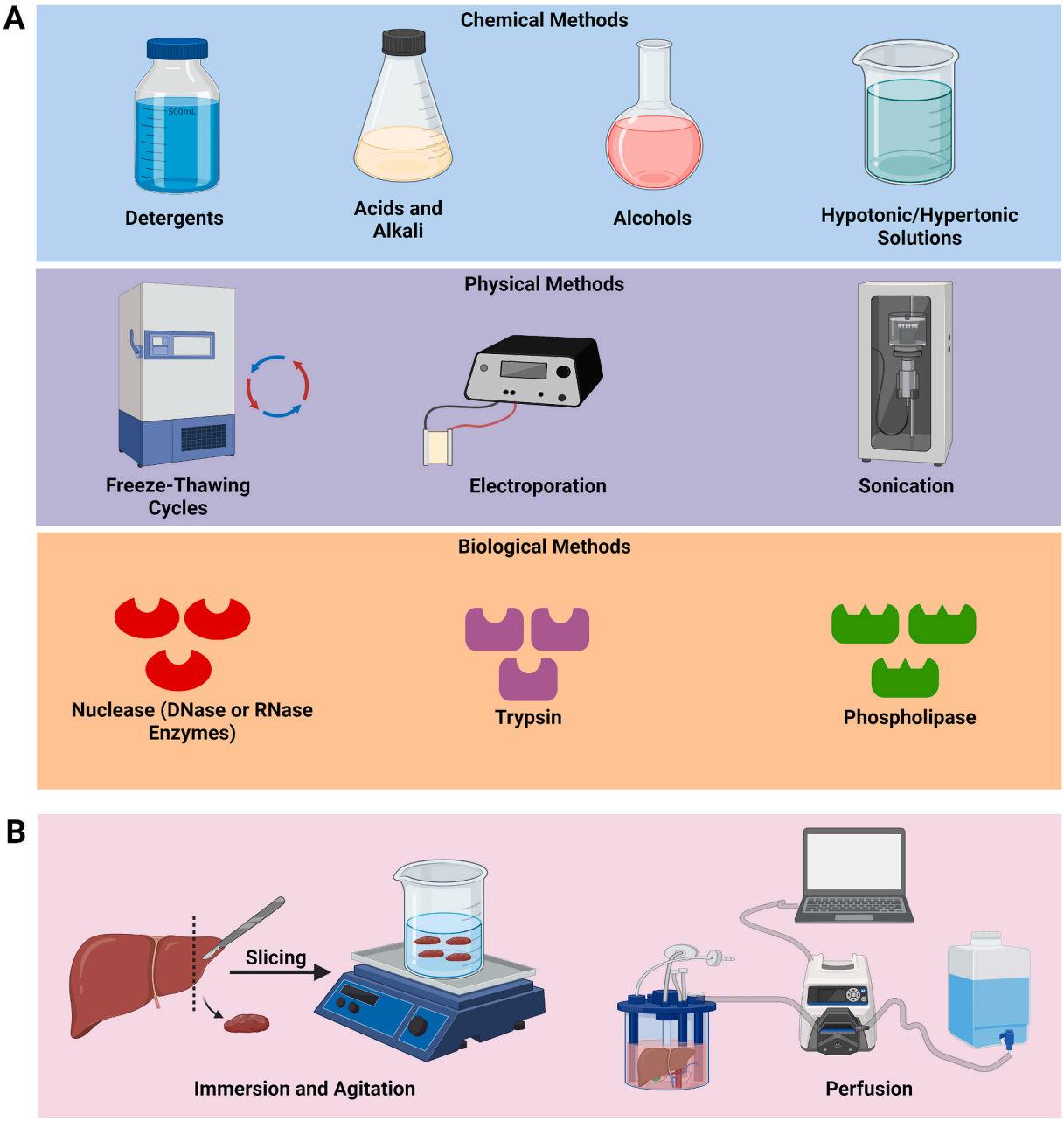

Fig. 2. Different decellularization agents (A) and techniques (B) for the fabrication of decellularized livers.

of biomolecules [59,102]. Peracetic acid (PAA) at a concentration of 0.1 % is the most commonly used acid for decellularization and sterilization of liver; however, it has adverse effects on GAGs, growth factors, and the mechanical characteristics of ECM [12,15,103–107]. Hussein et al. demonstrated that PAA was highly efficient at removing cellular material from the thin liver slices and was able to sterilize the scaffold [104]. Following PAA treatment, the decellularized liver retained 56 % of its GAGs content. Similarly, sodium hydroxide and ammonium hydroxide have been used in combination with detergents such as Triton X-100 and SDS to decellularize the liver with minimal detrimental effects on growth factors [11,13,22,108]. These alkaline agents can separate DNA strands at pH levels higher than 11, extract cell components, and considered cytocompatible for the subsequent recellularization process [102,109].

4.2.1.1.1.3. Alcohols

Alcohols, including ethanol and isopropanol, are commonly used to degrade and eliminate lipids from tissues by dehydrating the tissues and subsequently lysing cells [59]. Due to their strong bactericidal properties against Gram-positive, Gram-negative, and acid-fast bacteria, as well as lipophilic viruses, many researchers have employed ethanol for the decellularization and sterilization of the liver [10,108,110,111]. However, ethanol-based decellularization methods have drawbacks, including tissue fixation, damage to the ECM ultrastructure, and the precipitation of cellular proteins [104,112,113]. After precipitation, these proteins are no longer soluble and cannot be washed out, which can leave residual cellular proteins within the scaffold. This has been confirmed by proteomic analysis, which has identified numerous cellular proteins remaining in the scaffold following alcohol treatment [114].

4.2.1.1.1.4. Hypotonic/hypertonic solutions

Hypertonic solutions (e.g., sodium chloride) and hypotonic solutions (e.g., Tris-HCl) cause cell shrinkage or swelling due to osmotic pressure, ultimately leading to cell lysis and the removal of cellular components from the cells. They disperse the antigenic cellular remnants throughout

the tissue with minimal disruption of ECM architecture and composition [115–117]. The main advantage of these solutions is the ease of washing out from the tissue, as well as their ability to remove other residual decellularizing chemicals, thereby reducing toxicity and improving the biocompatibility of the decellularized tissue [118]. Although hypertonic solutions are efficient in removing proteins and hypotonic solutions are efficient in removing nuclei and DNA, they may not completely eliminate cellular residues and may require additional treatment to facilitate the removal of cellular debris [117,119,120]. Therefore, they could improve liver decellularization when used in combination with other chemical or enzymatic reagents. Kobes et al. reported that sequential agitation of mouse liver with a hypotonic solution followed by immersion in Triton X resulted in efficient decellularization, as confirmed by the absence of cells upon scanning electron microscopy imaging and retention of structural integrity [121].

4.2.1.1.2. Physical methods. Physical decellularization techniques involve the utilization of temperature, pressure, and other physical attributes to break down cell membranes and aid in the removal of cells from tissues or organs. Despite their low toxicity, these techniques are typically ineffective in completely eliminating all cellular components, resulting in retention of considerable amounts of immunogenic cell remnants within the decellularized material [5]. Therefore, they are commonly used as adjunctive treatments to complement the effects of chemical and biological agents, thereby enhancing the overall efficacy of the decellularization process.

4.2.1.1.2.1. Freeze-thawing

Freeze-thawing cycles induce the rupture of cell membranes and cell lysis within tissues and organs by forming ice crystals. Typically, the freeze-thawing cycle involves exposing the organ to freezing temperatures (−20 °C: −87 °C), followed by a range of 4 °C to normal biological temperature (4 °C–37 °C) [59,108,110,122,123]. Since no chemical or enzymatic reagents are used during the freeze-thawing procedure, this technique is considered safe due to the absence of residual chemicals and minimal impact on tissue structure and biochemical composition after decellularization [118,124–126]. Although freeze-thawing alone has been used to prepare cell-free matrices from tissues such as tendons and nerves, for whole organs like the liver, this method is typically combined with chemical or enzymatic treatments to remove membranous and intracellular contents [118,127,128]. One significant disadvantage of using freeze-thawing for liver tissues is the damage to the vascular architecture and duct structures, which can compromise the integrity and functionality of the decellularized scaffold. Several researchers have reported a detrimental effect of freeze-thawing, even with a single cycle, on the mechanical properties of the ECM, attributed to the formation of ice crystals and disruption of the ECM ultrastructure [129]. To mitigate ECM disruption and preserve the biomechanical performance of the organ, the use of cryoprotectants during the freeze-thawing process has been suggested. Pulver et al. demonstrated that pretreatment of rat liver with 5 % trehalose via perfusion for 30 min prior to freezing achieved comparable retention of ECM composition as in the control (overnight freeze-thaw cycle), but with reduced microstructural damage [130].

4.2.1.2.2.2. Sonication

Sonication involves the use of ultrasonic acoustic energy waves with frequencies greater than 20 kHz to induce cavitation, the formation and collapse of air bubbles in a liquid containing tissues or organs, typically achieved using an ultrasonic bath or probe [131]. During cavitation, these bubbles release shockwaves upon collapse, damaging cell membranes and facilitating the penetration of chemical detergents, thus expediting the removal of cellular debris. Therefore, production of more bubbles results in greater disruption of the cell membrane. However, excessive shockwaves and inappropriate acoustic power can potentially harm the tissue microstructure and decrease the efficiency of detergents in solubilizing cell membrane lipids. Additionally, heat generated during sonication, resulting from the friction of sound waves with the solution, can degrade the extracellular matrix (ECM), making temperature monitoring during sonication crucial [132–134]. Sonication has been employed by several researchers to prepare decellularized scaffolds from various tissues such as skin, cartilage, tendons, ligaments, larynx, ovaries, and blood vessels [132–137]. Thus far, ultrasonication has solely been employed in the decellularization of kidneys among whole solid organs, leading to a notable reduction in decellularization duration when combined with perfusion decellularization using SDS and/or Triton X [138]. To date, sonication has not been utilized in liver decellularization due to the liver's large size and dense composition, necessitating high power to disrupt its microstructure effectively.

4.2.1.2.2.3. Electroporation

Electroporation, a well-established biophysical technique, applies pulsed direct electric fields to increase cell permeability to ions and molecules by creating nanoscale pores in the lipid bilayer [7]. When the electric field surpasses a relatively high threshold (e.g., 700 V/cm for eight 100 μs pulses at 1 Hz in the liver), the cell membrane undergoes permanent changes in permeability, ultimately leading to cellular death, a process known as non-thermal irreversible electroporation (N-TIRE) [139]. This technique has been utilized for tissue and organ decellularization, including blood vessels, myocardium, and liver, both *in vitro* and *in vivo* [140–144]. Notably, N-TIRE does not require the use of chemicals or enzymes, thus avoiding any chemical or enzymatic residues.

Sano et al. utilized N-TIRE accompanied by lactated Ringer's solution perfusion through the portal vein and hepatic artery for porcine liver decellularization, facilitating the removal of cellular debris resulting from electroporation [139]. Golberg et al. successfully decellularized different zones of the rat liver *in vivo* by applying 90 unipolar, rectangular electric 70 μs pulses, at 150 Vmm−1 potential difference between the electrodes, at 4 Hz [140]. The treated areas showed rapid decellularization with preservation of the ECM structure. Similarly, Zhang et al. exposed the rat liver to a sequence of 10 square pulse with an electric field of 1000 V/cm, 100 μs pulse width, separated by 100 ms between the electrodes [145]. They achieved complete hepatocyte disintegration at 6 h post-treatment. Based on these studies, a limitation of electroporation is the small size of the probe, which restricts the area of decellularization.

4.2.1.1.3. Enzymatic methods. Enzymatic treatments using nucleases, trypsin, alpha-galactosidase, dispase, phospholipase, and collagenase are commonly employed methods for decellularization [7,146]. Despite the high specificity of enzymes in removing cell components by targeting specific bonds or interactions within cellular fragments or the cell-matrix, entirely decellularizing a whole organ using enzymes alone poses challenges. Additionally, the high cost of enzymes presents a barrier, as a substantial volume is required for the decellularization of large-scale livers [5]. Furthermore, enzyme residues may negatively affect the recellularization process or simulate an adverse immune response [147,148]. Hence, enzymatic treatment, particularly involving nucleases and trypsin, is often combined with chemical detergents followed by various washing cycles for liver decellularization [110,123,149,150].

4.2.1.1.3.1. Nuclease

Nucleases cleave the phosphodiester bonds between nucleotides of nucleic acids (DNA and RNA), facilitating the removal of nucleic materials following cell rupture [151]. Deoxyribonuclease (DNase), a common nuclease, is typically applied after chemical detergents to solubilize cell membranes and dissociate their inner structure, enhancing DNase infiltration and efficiency within tissues [152–154]. This combined approach has led to complete depletion of cellular and nuclear materials, with more than 95 % DNA removal [9,149]. Prolonged exposure to nucleases used in research settings, which may contain impurities, may negatively impact ECM structure and constituents, affecting the mechanical stability [152,153]. Moreover, extensive washing should be performed to rinse the decellularized organ and remove enzyme residues from the scaffold to prevent potential interactions between nucleases and reseeded cells [155]. Bühler et al.

studied the effect of DNase treatment on SDS-decellularized porcine liver, reporting a higher GAG content after DNase treatment alongside SDS perfusion compared to liver decellularized by SDS alone [149].

4.2.1.1.3.2. Trypsin

Trypsin catalyzes the hydrolysis of peptide bonds by cleavage of these bonds at the carboxyl side of lysine or arginine amino acids leading to dissociation of cellular components from the ECM [156,157]. Protease inhibitors released from damaged cells restrict the trypsin activity, particularly in prolonged trypsin treatment cycles, making it slow to remove cells. This necessitates periodic replacement of trypsin during the decellularization process [59]. Trypsin is disruptive to ECM components, especially collagen and elastin, potentially affecting mechanical strength, particularly with higher concentrations or longer exposure times [158–161]. Therefore, optimizing concentration and exposure time is critical.

4.2.1.3.2.3. Phospholipase

Phospholipases are lipolytic enzymes that cleave ester bonds within phospholipids, aiding in delipidation process [157]. Gessner et al. used phospholipase and nucleases (DNase and RNase) in combination with detergent for rat liver decellularization [162]. They also infused the liver with a high-salt buffer (NaCl) to preserve collagen and cytokine/growth factors bound to collagen. Their protocol yielded efficient decellularization while preserving the ECM ultrastructure and the macro- and micro-vascular network.

4.2.1.2. Methods of applying decellularization agents. These reagents are applied through either immersion and agitation or perfusion. Agitation is commonly employed for decellularizing liver slices to optimize the best decellularizing or sterilizing reagents [68,104]. For whole liver decellularization, perfusion is the commonly used technique.

4.2.1.2.1. Immersion and agitation. Immersion and agitation constitute a relatively straightforward decellularization method commonly used for thin tissues and smaller organs lacking vascular access, such as the esophagus, small intestine submucosa, urinary bladder, blood vessels, trachea, skin, cornea, and nerve [117,119,120,126,152,163–167]. This process involves submerging the tissue in a chemical or biological agent while subjecting it to constant mechanical agitation. This approach expedites cell disruption, detachment from basement membranes, removal of cellular components, ensures uniform exposure to decellularizing reagents, and achieves effective decellularization with reduced exposure time to harsh agents [157]. The decellularization efficiency relies on the decellularizing agent used, tissue thickness, duration of immersion, and intensity of agitation. Although immersion and agitation alone are insufficient for whole liver decellularization, they are suitable for decellularizing thin liver slices or cubes. This technique enables the production of a high number of slices or cubes, facilitating investigations into the effects of various decellularizing reagents, concentrations, and sterilization methods on the hepatic ECM [68,104]. For instance, Park et al. compared between five different solutions for decellularizing liver cubes: 0.1 %, 1 %, and 4 % SDS, 1 % Triton X-100, and a combination of 1 % Triton X-100 with 1 % SDS [68]. They reported that 0.1 % SDS effectively removed DNA and potential immunogenic and viral antigens from matrices while preserving 63 % of collagen and 71 % of GAGs compared to native liver. Upon subcutaneous implantation in pigs, the implanted decellularized tissues elicited minimal host responses and naturally degraded within 10 weeks. Similarly, Hussein et al. assessed the effects of sterilization with 0.1 % PAA, 70 % ethanol, and slightly acidic electrolyzed water (SAEW) on the ECM composition and biological activity of porcine liver decellularized with 0.1 % SDS. They observed that PAA and SAEW treatments yielded the highest sterilization efficiency and effectively removed a considerable amount of DNA from decellularized livers [104]. SAEW also retained more GAGs compared to other sterilization methods.

4.2.1.2.2. Perfusion. Perfusion, which involves the infusion of chemical or biological agents through the cannulated intrinsic vascular system, represents an ideal approach for decellularizing large, thick, compact organs like the liver [7,12]. This technique ensures the homogeneous spread and infiltration of decellularizing reagents throughout the entire tissue, facilitating the removal of cellular and nuclear material [168]. Perfusion-based decellularization has attracted significant attention because it enables the preservation of the three-dimensional ECM structure intact, which is crucial for producing clinically-scaled livers for human transplantation [169]. Moreover, perfusion retains the inherent vascular network (portal vein, hepatic artery, and hepatic veins), necessary for the transportation of nutrients and oxygen within liver during the recellularization process and post-transplantation *in vivo* [13,14,168]. Furthermore, the biliary tree is maintained post-perfusion decellularization, requiring only reseeding by cholangiocytes to restore functionality [110]. Importantly, the efficiency of decellularization via perfusion depends on various factors, including the route of perfusion (hepatic artery or portal vein or inferior vena cava), perfusion direction (antegrade or retrograde), perfusion conditions (controlled pressure and flow rate), duration of the perfusion, type and concentration of decellularizing agents, and the size of the liver [7,26,170]. Damage of the ECM due to inappropriate perfusion conditions, the requirement of vascular cannulation, and the need of specific perfusion pump with complex setups for flow control are the main drawbacks of the perfusion method [157].

4.2.2. Cross-linking

During recellularization and after *in vivo* transplantation, decellularized liver may undergo breakdown process known as "biodegradation" which affects negatively on the biomechanical strength of the ECM [5]. Cross-linking agents have been successfully employed to enhance enzymatic resistance, matrix decomposition, and ultimately improve biomechanical strength in various tissues and organs [171–173]. Additionally, cross-linking has been suggested to minimize potential immune responses against transplanted decellularized tissues by masking antigenic markers present in collagen [174,175]. Glutaraldehyde has been used as a potent cross-linking agent; however, it has several complications such as cytotoxicity and calcification [176]. Wang et al. used genipin, a naturally occurring cross-linking agent, for porcine liver cross-linking following perfusion decellularization with 1 % Triton X-100 and 1 % SDS [69]. They examined the biocompatibility of the scaffold by culturing human endothelial cells (EA.hy926) or primary rat hepatocytes on the cross-linked decellularized liver. Genipin cross-linking showed non-significant suppressive effects on the viability of primary hepatocytes and endothelial cells, unlike glutaraldehyde cross-linking, which displayed significant cytotoxicity. Upon implantation of the cross-linked scaffolds in a rat partial-thickness abdominal wall defect model, genipin-treated scaffolds elicited predominantly M2 macrophage phenotype responses, while glutaraldehyde-treated scaffolds resulted in disrupted host tissue remodeling and a mixed macrophage polarization profile. However, despite its biocompatibility and effectiveness, genipin's clinical applicability is limited due to the dark blue appearance of scaffold after treatment by genipin, high cost, and the complex extraction process [172].

Recently, the great interest in nanotechnology encouraged researchers to investigate the cross-linking effects of nanomaterials on decellularized tissues. Silver nanoparticle have been employed for cross-linking of porcine liver slices, preserving ultrastructure, enhancing resistance against *in vitro* degradation, and demonstrating good cytocompatibility with hepatocellular carcinoma cell line (HepG2 cells) and EA. hy926 cells [177]. Furthermore, silver nanoparticle-treated scaffolds exhibited reduced host inflammatory reactions and higher M2 macrophage polarization upon subcutaneous implantation in mice compared to glutaraldehyde and ethyl carbodiimide hydrochloride and N-hydroxysuccinimide-treated scaffolds [177]. In another study, Kim et al. perfused decellularized rat livers with nano-graphene oxide via both bile duct and portal vein for 24 h at 4 °C [178]. Nano-graphene oxide protected scaffold from *in vitro* degradation by directly

inhibiting matrix metalloproteinase activity and increasing mechanical rigidity. Subsequent subcutaneous implantation of cross-linked scaffolds promoted M2-like macrophage polarization, reducing graft-elicited inflammation. Interestingly, nano-graphene oxide-cross-linked livers were recellularized with endothelial and miHep cells and transplanted into acute (median and lateral lobe hepatectomy) and chronic (thioacetamide induced) liver failure mouse models, remaining functional post-transplantation.

4.2.3. Sterilization

Terminal sterilization of decellularized liver is a prerequisite for *in vitro* cell culture in a bioreactor and eventual *in vivo* implantation. The ideal sterilization agent/method should not only effectively kill or remove microorganisms, but also be safe, easy to use, and have minimal impact on the biocompatibility, physical or biological activity of the scaffold [104,179]. Therefore, the selection of a sterilization agent/-method is critical. Ethanol, PAA, slightly acidic electrolyzed water, PAA/ethanol, irradiation, and antibiotics have been used for sterilization of decellularized liver [9,13,104,110]. In one of our previous studies, we compared between 0.1 % PAA, 70 % ethanol, and slightly acidic electrolyzed water for sterilizing decellularized pig liver slices for 2 h [104]. Both SAEW and PAA effectively sterilized the scaffold without affecting the collagen, whereas ethanol decreased the collagen amount and did not efficiently sterilize the scaffold upon incubation in DMEM supplemented with 10 % FBS and on Columbia blood agar medium.

It has been reported that γ sterilization affects the scaffold's elasticity, subsequently affecting cell attachment, behavior, and viability [180–182]. Mirmalek-Sani et al. sterilized the whole decellularized porcine liver with 1 Mrad (10 kGy) γ irradiation, then reseed the scaffold with HepG2 cells. TUNEL assay indicated minimal apoptotic response of HepG2 cells to liver scaffolds, confirming the noncytotoxic effect of the scaffold [183]. Mattei et al. sterilized freeze-dried decellularized porcine liver discs by exposing them to chloroform vapor, H2O2 gas plasma, a combination of chloroform vapor and H2O2 gas plasma, or PAA, before performing direct contact cytotoxicity assay with hepatocytes for up to 48 h [184]. Chloroform vapor and immersion in PAA showed no cytotoxic effect on the hepatocytes, whereas H2O2 gas plasma treatment (with or without chloroform) showed a very toxic effect on hepatocytes. This may be attributed to the generation of free radicals after H2O2 treatment, which negatively affects the matrix.

4.2.4. Criteria for evaluating the fabricated liver scaffold

The protocols used for liver decellularization are quite variable from lab to lab, with the aim of preserving the ECM structure and bioactivity while removing cellular and nuclear material to avoid host responses after *in vivo* transplantation of the scaffold. Attaining this balance requires careful optimization of decellularization protocols to effectively remove cellular material while retaining essential ECM structures and bioactive molecules. Different factors influence this balance including the selection of decellularization agents, their concentrations, and the duration of treatment. Additionally, the mechanical forces applied during decellularization, such as agitation or perfusion, should be precisely controlled to minimize disruption to the ECM. For commercial production of liver scaffolds, a standardized, efficient decellularization technique should be applied. Following the preparation of the decellularized scaffold, the brown color would change into a pale or transparent white; however, this color change does not guarantee efficient decellularization of the scaffold. Initially, Badylak and his team suggested three necessary criteria to assure decellularization efficiency, based on various studies investigating *in vivo* remodeling and immune response [7]. The first criterion is the lack of nuclear materials in sections stained with 4', 6-diamidino-2-phenylindole (DAPI) or hematoxylin and eosin (H&E). The second criterion is the depletion of DNA from the ECM, with the scaffold containing less than 50 ng dsDNA/mg ECM dry weight, as quantified using commercially available dsDNA kits. The third criterion is that the DNA fragment length should be less the 200 bp, as determined by gel electrophoresis. DNA was initially used as an indirect measure of decellularization because it is challenging to remove. This difficulty made it a practical way to assess how thoroughly cells had been removed from a scaffold. However, it is now recognized that DNA content is not a robust indicator of decellularization efficiency or scaffold safety, as the FDA does not require DNA content specifications due to confidential product safety data submitted by manufacturers. From our experience in the field of decellularization, we recommend evaluating the absence of the alpha-Gal by PCR, immunostaining, or ELISA quantification to confirm the complete depletion of alpha-Gal. Additionally, due to the risk of zoonotic transmission of porcine endogenous retrovirus (PERV), it is critically important to ensure the complete absence of PERV by PCR within the decellularized porcine liver [5]. Moreover, it is equally important to investigate the retention of key ECM components, including collagen, GAGs, and growth factors, which are necessary for preserving the structural integrity and biological function of the tissue.

Importantly, most decellularizing agents have a cytotoxic effect even at very low concentrations, so confirming the complete rinsing of the decellularized liver from these agent residues is essential [59,185]. Different methods have been used to measure the residues of decellularizing agents qualitatively or quantitatively after completing the decellularization process. This is critical to avoid cytotoxicity resulting from the toxic effects of the agents, as well as to optimize sufficient time for washing the decellularized scaffolds to guarantee their biocompatibility [5]. Moreover, retention of chemicals such as SDS has been reported to promote inflammation and foreign body reactions [92,186]. Methylene blue dye-binding assay is commonly used to quantify SDS using digested scaffolds [187]. Visible light spectroscopy has also been described as a simple method for detecting/quantifying trace amounts of SDS. This method relies on the utilization of a carbocyanine dye, Stains-All, which undergoes a color change from intense fuchsia to yellow with the addition of SDS [91,188]. Gas chromatography has been used to quantify the residual amount of SDS after decellularization of porcine liver slices [68]. Additionally, C14-labeled SDS was used to quantify the residual SDS present within decellularized human amniotic membrane [100]. Importantly, residual SDS was detected in both the final wash buffer (3.01 ± 2.72 μg/ml) and the decellularized amniotic membrane (0.62 ± 0.13 μg/mg). Interestingly, this low concentration was shown not to affect the viability of primary human dermal fibroblasts and primary human dermal keratinocytes cultured on the decellularized amniotic membrane.

Given that cytotoxicity could occur even at very low concentrations of decellularizing agents and may inhibit or completely kill the reseeded cells and negatively affect the ECM, new methods to detect and quantify the different residual decellularizing agents within the scaffolds are required. These methods should be simple, accurate, have low detection limits and large calibration ranges, and short analysis times.

4.3. Reconstruction of the parenchymal regions

Recellularization is defined as implanting specific cell types into the decellularized tissue to form an engineered construct with specific structures and functions that mimic the original tissue. This process consists of two main steps: the first is seeding the cells, allowing them to distribute to the appropriate locations within the decellularized liver scaffold. The second step involves perfusion of the whole liver through the main vessels with culture media under physiological conditions to simulate the *in vivo* state. The liver is composed of heterogeneous cell types, including hepatocytes, biliary epithelial cells (cholangiocytes), endothelial cells, stellate cells, Kupffer cells, progenitor cells, and undifferentiated cells [189]. Therefore, constructing a transplantable and functional bioengineered liver demands these different cells to repopulate not only the parenchymal space, but also the vascular lining, sinusoids, and biliary network.

In the context of liver transplantation, several studies have suggested that transplanting approximately 20–30 % of the normal liver mass can

provide sufficient function for the recipient. For instance, a human weighing 70 kg would require approximately 84 billion hepatocytes to attain at least 30 % liver function [190,191]. So, theoretically, incomplete repopulation of the liver parenchyma within the decellularized scaffold might be sufficient, as the reseeded hepatocytes can proliferate *in vivo* to fill the parenchyma [192]. Nevertheless, this hypothesis lacks conclusive evidence.

Several studies have been conducted to evaluate the feasibility of recellularizing decellularized livers, primarily on rodent liver initially, and researchers have continued to scale it up using whole porcine and human livers (Table 1) [8,14,101,110,193–195]. This has led to have different cell sources and various strategies for recellularization with improved repopulation efficiency. These recellularization strategies are mainly adaptations of the techniques applied for traditional cell culture, tissue engineering, cell transplantation therapies, and isolated organ perfusion [196].

4.3.1. Cell source

4.3.1.1. Primary hepatocytes. Primary human hepatocytes are the preferred candidate for repopulating bioengineered livers for clinical use due to their high host compatibility. However, primary human hepatocytes are scarcely available, and are primarily sourced from discarded cadaveric liver samples. Moreover, they have short life spans, poor proliferative capacity, and rapid loss of liver-specific function and morphology [197]. Porcine hepatocytes have been explored as an alternative to primary human hepatocytes in different recellularization trials. Yagi et al. reseeded decellularized porcine livers with primary porcine hepatocytes and perfused media via the portal vein at 4 ml/min, with a partial oxygen tension of approximately 300 mmHg [198]. Importantly, they reported that around 47.8 % of reseeded hepatocytes were apoptotic by day 7. Furthermore, they observed that albumin immunostaining was lower after 7 days of media perfusion compared to day 4, attributed to shear stress caused by media flow.

Anderson et al. demonstrated that both primary hepatocytes, when cultured alone or co-cultured with human umbilical vein endothelial cells (HUVECs), exhibited substantial ammonia clearance and urea release, indicating the ability of hepatocytes to retain their function in high-density cultures within decellularized porcine liver scaffolds [193].

Porcine primary hepatocytes have drawbacks that could hinder their potential application in clinic, such as the potential immunogenic reaction induced by proteins produced by porcine cells and the risk of transferring viral pathogens, such as PERV, porcine cytomegalovirus, and porcine lymphotropic herpesvirus [199–202].

Primary murine hepatocytes are frequently used for recellularization experiments and have demonstrated the ability to attach, grow, proliferate, and survive within decellularized rodent livers while retaining their morphology and function [12,110,203].

4.3.1.2. Human hepatocyte cell lines. To address the challenges associated with using primary hepatocytes, tumor-derived hepatocyte cell lines such as HepG2 cells have been widely used to repopulate the parenchymal space of decellularized livers. This choice is favored due to the advantages of availability, rapid growth allowing for inexpensive expansion to attain sufficient cell numbers for recellularization, and secretion of human proteins. HepG2 cells efficiently repopulate decellularized rat, porcine, and human livers while retaining their function and proliferative capacity [14,15,204].

HepG2 cells exhibit higher expression of functional genes, including albumin, low-density lipoprotein receptor (LDLR), and CYP2E1, as well as increased albumin secretion when cultured following efficient reendothelization and coating of the vascular tree with a heparin-gelatin mixture compared to uncoated reendothelized porcine liver [14]. This emphasizes the importance of efficient reendothelization in protecting parenchymal cells from shear stress caused by media perfusion and enhancing hepatocyte function. However, from a clinical standpoint, HepG2 cells are not a good option for clinical use due to their tumorigenicity and lack of normal metabolic profiles, particularly ureagenesis, compared to primary hepatocytes [205].

4.3.1.3. Human fetal hepatocytes. Human fetal hepatocytes (Hfh) are considered an alternative cell source for recellularization due to their proliferative and functional capacities [23]. Importantly, these cells are not genetically modified, thus carrying a lower risk of tumorigenicity than hepatoma cell lines or immortalized human cell lines. Additionally, there is no risk of zoonotic transmission and immunological issues often associated with xenogeneic hepatocytes [206,207].

Human fetal hepatocytes were able to repopulate decellularized porcine liver when co-cultured with fetal stellate cells after a 13-d perfusion period, with 70 % of the cells staining positive for albumin. Interestingly, the expression declined as the perfusion period progressed. Immunohistochemical staining demonstrated decreased expression of alpha-fetoprotein (AFP) and CYP3A7 and increased expression of CYP3A4, cytokeratin (CK)-18, and periodic acid-Schiff (PAS), indicating promising maturation of Hfh as the perfusion progressed [23].

The main challenges regarding the use of human fetal hepatocytes are their availability, ethical concerns, and incomplete functional maturity of the fetal cells [207,208].

4.3.1.4. Mesenchymal stem cells. Mesenchymal stem cells (MSCs) can be obtained from different sources such as bone marrow and adipose tissue. Autologous MSCs are considered as a potentially clinically relevant cell type for hepatic tissue engineering due to their availability, expandability, and safety profile, along with possible beneficial immune modulation effects [209,210]. Jiang et al. reseeded the decellularized mouse liver with MSCs derived from mouse bone marrow via the portal vein and induced their differentiation towards the hepatic lineage during media perfusion [211]. The three-dimensional environment of the decellularized liver supported the hepatic differentiation of MSCs, as evidenced by higher expression levels of hepatic-specific genes and marker proteins, increased glycogen storage, albumin secretion, and urea production compared to cells differentiated in 2D cultures.

4.3.1.5. Induced pluripotent stem cells. Induced pluripotent stem cells (iPSCs) are a type of pluripotent cells that can be produced by reprogramming human or animal differentiated adult cells via overexpression of four transcription factors: Oct 4/3, Sox 2, Klf4 and c-Myc [212]. These cells can then be redifferentiated into hepatocyte-like cells. Park et al. produced the porcine iPSCs from ear skin fibroblasts and differentiated them into hepatocytes (iPSCs-Hep) using solubilized decellularized porcine liver extract [213]. The iPSCs-Hep were then reseeded into a decellularized rat liver through the portal vein and distributed well within the parenchyma of the scaffold, exhibiting the ability to secrete albumin and urea into the perfusate.

Similarly, Minami et al. recellularized a rat liver scaffold with hepatocyte-like cells derived from human iPSCs (hiPSCs) via the biliary duct [214]. The repopulating cells secreted albumin and stained positive for albumin, AFP, and CYP3A4 after 48 h of media perfusion. The expression of AFP suggested insufficient maturation of the engrafted cells.

To evaluate the ability of the microenvironment, including the unique composition and native 3D organization within the decellularized liver ECM, to induce the differentiation, Acun et al. reseeded a rat liver scaffold with undifferentiated iPSCs [215]. After 7 days of media perfusion, the iPSCs differentiated into hepatocyte-like cells, showing higher expression of mature markers, including CYP450 enzymes, albumin, and HNF4a, compared to hepatocyte-like cells produced in a 3D geltrex matrix.

The advent of induced pluripotent stem cell (iPSC) technology has paved the way for using patient-specific iPSC-derived hepatocytes (iPSC-

Table 1
Summary of studies reported the decellularization and recellularization of the liver scaffolds with different cells.

Source	Decellularization method	Sterilization method	Cell type/Seeding route/ reendothelization enhancement	In vitro culture	In vivo Transplantation	Main outcomes	Ref.
Rats	−0.01 % SDS for 24 h −0.1 % SDS for 24 h −1% SDS for 24 h −1% Triton X-100 for 30 min - Via portal vein	0.1 % peracetic acid for 3 h	- Primary rat hepatocytes and rat cardiac microvascular endothelial cells via portal vein	Dynamic for 5 d	Heterotopic transplantation of the median lobe for 8 h after unilateral nephrectomy.	1 Successful decellularization with preservation of ECM components was confirmed by H&E, immunohistochemistry, and SEM. 2 Reseeded cells were functional (albumin secretion, urea synthesis and cytochrome P450 expression at comparable levels to normal liver *in vitro*). 3 Hepatic function (albumin, G6pc and Ugt1a) was also retained in the transplanted grafts, with minimal indications of ischemic damage.	Uygun et al. [12]
Rats	−1%, 2 %, 3 % Triton X-100 for 1 h each −0.1 % SDS for 1 h - Via the inferior vena cava	Decellularization solutions contained 1 % antibiotic/ mycotic	Rat liver progenitor cell line WB344 via the inferior vena cava	Not mentioned	–	1 0.1 % SDS for 1 h completely removed all DNA. 2 Addition of antibiotics/ antimycotics to all perfusion solutions prevented microbial growth. 3 Reseeded cells distributed within the center of the scaffold.	Shupe et al. [21]
Rats	- Freeze-thawing −0.02 % trypsin/ 0.05 % EGTA for 2 h −3% Triton X-100/0.05 % EGTA for 18–24 h - Via IVC	−0.1 % peracetic acid/4 % EtOH for 1 h. - Terminal sterilization by 2MRad gamma irradiation	- Primary mice hepatocytes via: (1) Direct parenchymal injection; (2) Continuous perfusion via the portal vein; and (3) Multistep infusion via the portal vein	Dynamic for 7 days	–	1 Decellularization process preserved the 3-D structure, the ultrastructure, the ECM components, the microvascular network, and the bile drainage system, and up to 50 % of growth factor content. 2 Multistep infusion technique of hepatocytes resulted in ~90 % of cell engraftment and provided the highest liver-specific functional capacities of the engrafted cells.	Soto-Gutierrez et al. [110]
Rats	−1% SDS, 0.5 % SDS, and 0.25 % SDS for 4 h each −1% Triton X-100 for 1 h - Via portal vein	- Antibiotic-containing saline for 72 h.	- Primary rat hepatocytes via the portal vein (from spheroid culture). - Scaffolds treated for heparin immobilization (layer-by-layer heparin self-assembly technique).	- Static for 4 h. - Dynamic for 2 h.	Heterotopic into 90 % hepa- tectomized rat portal system for 72 h.	1 Treating hepatectomized rats with a recellularized liver scaffold improved liver function and prolonged survival. The mean lifespan was extended from 16 to 72 h. 2 At 72 h post operation, the recellularized scaffold maintained the functionality and viability of hepatocytes.	Bao et al. [218]
Ferret	−1% Triton X-100 + 0.1 % ammonium hydroxide - Via portal vein	−1.5MRad gamma irradiation	- Human foetal liver cells + HUVECs endothelial cells co-infusion via the portal vein over a period of 16 h.	Dynamic for 7 days	Heterotopic transplantation of decellularized right lobe for 1 h.	1 Cells repopulated in their native locations within the decellularized scaffold and displayed typical endothelial, hepatic, and biliary epithelial markers, thus creating a liver-like tissue *in vitro*.	Baptista et al. [13]
Rats	Two decellularization protocol: −1% SDS for 2 h −1% Triton X-100 + 0.05 % sodium hydroxide for 2 h - Via portal vein	–	Primary rat hepatocytes via the portal vein	Dynamic for 7 days	–	1 Collagen preservation was observed in both protocols. - Elastin decreased to around 20 % and 60 %, GAGs to about 10 % and 50 %, and hepatocyte growth factor (HGF) to roughly 20 % and 60 % of their original levels in the native liver following	Ren et al. [101]

(*continued on next page*)

Table 1 (*continued*)

Source	Decellularization method	Sterilization method	Cell type/Seeding route/ reendothelization enhancement	In vitro culture	In vivo Transplantation	Main outcomes	Ref.
						SDS and Triton X-100 treatments, respectively. 2 Triton X-100-treated scaffolds showed significantly better support for liver-specific functions, such as albumin secretion, urea synthesis, ammonia elimination, and mRNA expression levels of drug metabolism enzymes, compared to SDS-treated scaffolds.	
Rats	- Freeze-thawing - Trypsin and Triton X-100 with EGTA, via SHVC for 24 h	–	Bone marrow MSC and primary rat hepatocytes via the portal vein. −3 × 10^8, 1 × 10^8, and 5 × 10^7 of hepatocytes together with 20 % of MSCs were infused in sequential order of Group 1: hepatocytes initially, Group 2: MSCs initially, and Group 3: hepatocytes and MSCs together.	Dynamic for 6 days	2 tubes were inserted into the portal vein and SHVC then connected to the recipient's left portal vein and left renal vein, respectively for 1 h.	1 Separate infusions of the two cell types resulted in higher numbers of hepatocytes and MSCs stacked inside the vascular walls, which reduced hepatocyte migration into and repopulation of the parenchymal space. 2 MSCs were well-engrafted among clusters of hepatocytes as well as inside the decellularized vascular walls in the matrix in Co-infusion at the same time. 3 Administration of MSCs into the scaffold enriched the microenvironment for factors related to hepatic regeneration and served as supportive cells for hepatocyte maintenance and protein production.	Kadota et al. [123]
Porcine	- Freeze-thawing −1% SDS for 22 h - DNase for 2 h - Via portal vein	–	Porcine hepatocytes via the portal vein	Dynamic for 2 days	–	1 Porcine liver were completely decellularized in a mean time of 24 h, as proven by a negative H&E staining and significantly decreased DNA levels. 2 Reseeded hepatocytes engrafted successfully in the liver scaffold with the ability to proliferate.	Bühler et al. [149]
Human	- Freeze-thawing. −0.025 % Trypsin-EDTA −0.01 % SDS, 0.1 % SDS, and 1 % SDS −3% Triton X-100 - Via portal vein	−5% Antibiotic and Antimycotic. −0.1 % PAA and 4 % ethanol.	Human cell lines hepatic stellate cells (LX2), hepato-cellular carcinoma (Sk-Hep-1) and hepatoblastoma (HepG2) via suspension	Static on liver cubes for 21 days.	Subcutaneously or into the omentum in immune competent mice for 21 days.	1 Cells grown on the liver cubes have excellent viability, motility, and proliferation. 2 No foreign body response was observed after *in vivo* implantation of the decellularized scaffolds.	Mazza et al. [15]
Rats	−0.1 % SDS for 60–80 min	−0.1 % peracetic acid for 2 h	- Hepatic carcinoma cells (HepG2)	Dynamic for 10 days	–	1 HepG2 cells exhibited robust growth on the scaffolds. 2 PCR indicated that cells maintained their functionality and invasion ability at significantly higher levels compared to cells cultured on 2D dishes or spheroids on Matrigel. 3 Cells grown on scaffolds responded to the drug (methotrexate) in a manner similar to its known activity *in vivo*.	Hussein et al. [204]
Piglet	−1% Triton X-100 and 0.1 % ammonium hydroxide for 2–3 days	−1.2 MRad gamma irradiation	- Murine endothelial cells (MS1) via the PV, HA, SH-IVC, and IH-IVC.	- Static for 1 h, followed by another 1 h infusion performed	Heterotopic transplantation of for 24 h after unilateral nephrectomy.	1 The conjugation of anti-CD31 antibodies to the vascular surfaces significantly enhanced the efficiency of reendothelization,	Ko et al. [11]

(*continued on next page*)

Table 1 (*continued*)

Source	Decellularization method	Sterilization method	Cell type/Seeding route/ reendothelization enhancement	In vitro culture	In vivo Transplantation	Main outcomes	Ref.
			- *Anti*-mouse CD31 antibodies were conjugated onto the vascular surfaces	following a 180-degree rotation of the liver scaffold from the original position. - Dynamic for 3 days.		leading to consistent endothelial attachment throughout the liver vasculature and extending to the capillary bed of the liver scaffold. This approach substantially decreased platelet adhesion during blood perfusion *in vitro*. 2 After transplantation, the reendothelialized livers were able to withstand physiological blood flow for up to 24 h	
Porcine	- Freeze-thawing −1% Triton X-100 for 3 h −1% SDS for 6 h followed by1% Triton X-100 for 3 h - Via portal vein	–	- Rat primary hepatocytes and human umbilical vein endothelial cells. - Scaffolds treated for heparin immobilization (layer-by-layer heparin self-assembly technique).	- Static on scaffolds specimen for 3 days.	Orthotopic transplantation for 1 h in the infrahepatic space after resection of recipient the right and left liver lobes.	1 The decellularized liver was depleted from PERV as assessed by PCR. 2 The heparinized scaffolds demonstrated improved anticoagulation as shown upon platelet adhesion and activation assays. 3 The heparinized scaffolds were biocompatible.	Bao et al. [219]
Rat	−0.02 % EGTA for 30 min −1% Triton X-100/0.1 % ammonium hydroxide for 20 h - Via portal vein	−0.1 % peracetic acid for 3 h	Rat normal liver cell line BRL were introduced by 2 methods: multi position parenchymal injection method or infusion method Via portal vein. - Endothelial progenitor cells infusion via portal vein (Separate culture)	- Dynamic for 7 days (for rat normal liver cell line BRL). - Dynamic for 3 days (for EPC)	Subcutaneously (Samples of decellularized scaffold were cut as 5 mm in diameter and 3 mm in thickness) for 21 days	1 Heterologous transplantation showed good biocompatibility of the scaffold. 2 BRL cells attached and functioned well in the scaffold. 3 EPCs covered the internal surface of the tubular structures in the scaffold.	Zhou et al. [105]
Porcine	−0.1%SDS for 9 h ± 2.5 h - Via the portal vein	0.1%PAA for 2 h.	- Hepatic carcinoma cells (HepG2) and human endothelial cells (EA.hy926) - Via the portal vein. - The vascular surfaces were coated by heparin-gelatin mixture.	- Dynamic for 10 days.	Orthotopic transplantation for 1 h after unilateral nephrectomy.	1 Heparin-gelatin mixture improved ECs attachment and migration toward vascular surface. 2 Decellularized liver repopulated endothelial cells after heparin gelatin coating revealed improved *ex vivo* blood perfusion compared to uncoated scaffolds. 3 In vivo results showed no coagulation occurred and parenchymal cell functions were maintained.	Hussein et al. [14]
Rats	- Freeze-thawing. −0.02 % trypsin/ 0.05 % EGTA for 1 h −1% Triton X-100 for 18–24 h - Via portal vein	0.1%PAA for 2 h.	- Adult and foetal mouse hepatocytes. - via the bile duct or the portal vein	- Dynamic for 7 days	–	1 Recellularization through bile duct showed a higher parenchymal distribution efficacy (80 %) compared to 20 % following portal vein seeding.	Ogiso et al. [217]
Rats	−0.1 % SDS for about 24 h - Via portal vein	–	HepG2 cells infused through the bile duct with either HUVECs via the portal vein or rat neonatal cell slurry infused via the bile duct.	Dynamic 5–7 days	–	1 HepG2 cells cocultured with HUVECs showed viable human endothelial lining with hepatocyte growth. In the neonatal cell slurry infusion group, distinct foci of hepatocytes were observed to repopulate the parenchyma of the scaffold with presence of cholangiocytes as verified by CK-7 positivity. 2 Albumin production was higher than that observed in traditional cell culture.	Hassanein et al. [194]

(*continued on next page*)

Table 1 (*continued*)

Source	Decellularization method	Sterilization method	Cell type/Seeding route/ reendothelization enhancement	In vitro culture	In vivo Transplantation	Main outcomes	Ref.
Rats	−0.02 % trypsin/ 0.05 % EGTA for 1 h −1% Triton X-100/0.05 % EGTA for 18–24 h - Via portal vein	0.1%PAA for 2 h.	1 Primary rat hepatocytes via the bile duct. 2 Liver sinusoidal endothelial cells (LSECs) or HUVECs via the portal vein	- Dynamic for 7 days	–	1 Seeding through biliary duct facilitated proper distribution of hepatocytes throughout the parenchymal space, while portal vein-seeded LSECs concurrently lined the portal lumen, thereby preserving function and morphology. 2 Hepatocytes co-seeded with LSECs retained their function compared to those seeded independently. 3 Platelet deposition significantly decreased, and hepatocyte viability was maintained in the co-seeded group following 8-h of extracorporeal blood perfusion.	Kojima et al. [195]
Rats	- Freeze-thawing. −0.01 % SDS −0.1 % SDS for 4 h −0.2 % SDS for 1 h −0.5 % SDS for 1 h −1% Triton X-100 for 30 min - Via portal vein	0.1 % PAA and 4 % ethanol.	- Human EA.hy926 endothelial cells. - Via the portal vein - REDV-ELP peptide was conjugated to the vascular surface.	- Dynamic for 4 days	–	1 REDV-ELP increased EC attachment and proliferation within the scaffold with uniform endothelial lining of the vasculature. 2 REDV-ELP conjugation reduced platelet adhesion and activation following *ex vivo* perfusion using platelet-rich plasma for 1 h.	Devalliere et al. [10]
Rats	- Freeze-thawing −0.05 % trypsin/ 0.05 % EGTA solution for 2 h −0.5 % Triton X-100/0.05 % EGTA for 3–12 h - Via portal vein	–	- HUVECs endothelial cells. - Via portal vein. - To improve cell adhesion properties, scaffolds were immersed in fibronectin solution before reendothelization.	- Static for 2 days. - Dynamic for 2 days with different flow rates	–	1 Perfusion culture enhanced the formation of sinusoid-scale microvessels in the scaffolds, which was not observed in static culture. Particularly, perfusion culture at 4.7 ml/min enhanced the formation of sinusoid-scale microvessels compared to perfusion culture at 2.4 and 9.4 ml/min 2 fibronectin coating stimulated the generation of sinusoid-scale microvessels during perfusion culture at 4.7 ml/min.	Watanabe et al. [150]
Rats	- Freeze-thawing −1% Triton X-100 with 0.1 % NH4OH for 3 h - Via portal vein	−0.1 % PAA in 4 % ethanol for 40 min. −0.1 % PAA for 30 min. - Antibiotic (penicillin/ streptomycin)	- Rat sinusoidal endothelial cells. - Via the portal vein. - Cell were injected in 5 % gelatin hydrogel solution for improving the attachment.	- Dynamic for 2 days	Heterotopic transplantation for 8 days	1 Gelatin hydrogels-based perfusion significantly increased the retained ECs within the scaffold which lined the vascular lumen and actively proliferate. 2 Doppler ultrasound showed active blood flow within the reendothelialized liver scaffold transplants after 8 days.	Meng et al. [108]
Rats	−0.01 % SDS for 24 h −0.1 % SDS for 24 h.-0.2 % SDS for 3 h.-0.5 % SDS for 3 h −1% Triton X-100 for 30 min - Via portal vein	−0.1 % PAA and 4 % ethanol for 3 h. - Antibiotics (penicillin, streptomycin and gentamicin) and antimycotic (amphotericin B)	- Rat cholangiocytes via the common bile duct. - Rat hepatocytes via the portal vein	- Dynamic for 2 days	–	1 Co-seeded scaffold with cholangiocytes through the biliary duct, alongside perfusing hepatocytes through the portal vein resulted in organization of the cholangiocytes into duct-like structures, while viable hepatocytes clustered in the parenchymal space, closely mimicking the arrangement found in native tissue. 2 Co-seeded scaffold had higher production of albumin and urea than grafts	Chen et al. [111]

(*continued on next page*)

Table 1 (*continued*)

Source	Decellularization method	Sterilization method	Cell type/Seeding route/ reendothelization enhancement	In vitro culture	In vivo Transplantation	Main outcomes	Ref.
						with hepatocytes only (not significant difference).	
Rats	- Freeze-thawing −0.02 % trypsin/ 0.05 % EGTA for 1 h −1% Triton X-100/0.05 % EGTA for 18–24 h - Via portal vein	−0.1 % PAA for 2 h.	- Human induced pluripotent stem cells derived hepatocyte-like cells. - Via bile duct	- Dynamic for 2 days	–	1 The hiPSC-HLCs distributed into the parenchymal space of the recellularized liver. 2 The recellularized liver expressed the albumin and CYP3A4 genes, and secreted human ALB into the perfusate.	Minami et al. [214]
Porcine	−1% Triton X-100 for 2–5 h −0.6 % SDS for 4–8 h - Via portal vein	−0.1 % PAA for 2 h.	- HUVECs endothelial cells via the superior vena cava followed by via the portal vein after 24 h.	Dynamic for 20 days	Heterotopic 20 days in immunosuppressed pigs	1 Implementing a 10-day steroid-based immunosuppression protocol along with splenectomy at the time of reendothelialized scaffold implantation reduced the immune responses and resulted in continuous perfusion of the scaffold for over two weeks. 2 HUVECs were localized within sinusoidal regions upregulated the expression of sinusoidal endothelial markers similar to those in normal liver tissue.	Shaheen et al. [8]
Porcine	−1% Triton X-100 for 2–5 h −0.6 % SDS for 4–8 h - Via portal vein	−0.1 % PAA for 2 h.	- HUVECs endothelial cells via the vena cava followed by the portal vein after 24 h. - Porcine hepatocytes via the bile duct typically 13–16 days following the first HUVEC seeding.	Dynamic for 20 days	Heterotopic in a pig model of surgically induced acute liver failure for 2 days.	1 Repopulated hepatocytes in the parenchymal regions reconstituted hepatic function within the scaffold as measured by albumin secretion, urea production, and ammonia clearance *in vitro*. 2 Co-seeded scaffolds showed improved biochemical function in an acute liver failure model.	Anderson et al. [193]
Rats	−0.1 % SDS for 6 h - DNase for 1 h - Via portal vein	−0.1 % PAA - Antibiotics	- Hepatic carcinoma cells (HepG2) via the bile duct twice with 48 h interval. - HUVECs endothelial cells were infused via the bile duct after 14 days of HepG2 culture. - *Anti*-CD31 aptamer was conjugated to the vascular surface.	Dynamic for 21 days	Transplantation in 2 models - Heterotopic in healthy rats for 2 h. - Into the interlobular space of the liver after removing the fibrous capsule for 4 weeks	1 Successfully coating the vascular surface of the scaffold with the Anti-CD31 aptamer led to enhanced endothelial cell coverage. 2 This modification allowed for perfusion with blood for 2 h, resulting in decreased platelet adhesion *ex vivo*. Additionally, in a hepatic fibrosis rat model, it effectively restored liver function.	Kim et al. [9]

Heps) for recellularization of decellularized livers for clinical applications. iPSCs offer an unlimited cell source and are less immunogenic, thereby avoiding the high cost and serious side effects associated with immunosuppression needed for allogenic cells. However, critical safety concerns remain regarding the use of viral vectors and the potential for teratoma formation, limiting the clinical application of iPSCs [197,216].

4.3.2. Methods of recellularization

Reseeding cells into decellularized liver can be achieved through direct injection into the parenchyma or through perfusion via the hepatobiliary vasculature. Given that the liver's primary blood supply is through the portal vein, which has a wide lumen and extensive branching, the latter approach is commonly used for hepatocyte seeding. Zhou et al. conducted a study comparing the repopulation efficiency of buffalo rat liver (BRL) epithelial-like cells after intraparenchymal injection or portal vein infusion [105]. They injected the cells into 10 sites within the parenchyma of decellularized rat liver or infused them into the portal vein. Cells delivered via portal vein infusion resulted in a low engraftment rate (83.4 % ± 5.2 %) and poor distribution of the seeding cells, whereas parenchymal injection resulted in a high engraftment rate (93.2 % ± 4 %) and better distribution of cells in the parenchymal space after 24 h. This difference was attributed to the tendency of reseeded cells to block the portal vein lumen and be washed out of the scaffolds.

Few studies have compared the effectiveness of seeding cells via the portal vein, bile duct, and vena cava. For instance, in a study by Ogiso et al., it was reported that there was significantly higher hepatocytes parenchymal engraftment when infused via the biliary tree compared to the portal vein [217]. The use of the vena cava (inferior/superior) for hepatocyte recellularization is less common. Shupe et al. reseeded the decellularized liver through the inferior vena cava using the rat liver progenitor cell line WB344, which spread into the center of the scaffold [21]. The authors did not specify the rationale behind recellularization via the vena cava.

To mitigate the risk of reseeded cells remaining in the vessel and causing blockage due to the use of a large number of cells, cell introduction into the scaffold can be performed through different injection approaches, such as multi-step infusion, or in a continuous perfusion manner. For example, Soto-Gutierrez et al. demonstrated that a multi-step infusion of cells via the portal vein resulted in a better parenchymal repopulation rate, with a cell engraftment rate of approximately 90 %, and exhibited higher proliferative capacity as well as a superior functional profile of engrafted cells, including albumin production, CYP1A1/2 activity, and ammonia clearance, compared to direct parenchymal injection and continuous perfusion [110].

4.4. Vascular reconstruction

During the decellularization process, the endothelial cell layer is typically removed along with other parenchymal cells. The ECM components, especially collagen present in the scaffold, can stimulate the activation pathway upon contact with circulating platelets in the bloodstream [150,220,221]. As a result, platelet aggregation and coagulation are expected to occur immediately after *in vivo* transplantation of the liver scaffold, potentially impeding the blood supply to the organ and causing cell death. Therefore, reconstruction of the vascular network becomes necessary to allow the perfusion of the graft with host blood, ensuring the supply of nutrients and oxygen to different regions of the bioengineered organ [14,222]. Generally, it has been reported that cells can only survive within an area approximately 1–3 mm away from a source of nutrients and oxygen [223]. Oxygen is crucially supplied to hepatocytes by the mixing of arterial (hepatic artery) and venous blood (portal vein) in sinusoids at a rate of ~1.2 nmol/s/10^6 cells to meet the oxygen demand and support the high metabolic activity of hepatocytes [224]. Considering this, inefficient reendothelialization may result in necrosis-induced death, accompanied by poor performance of the graft and potential rejection.

Vascular reconstruction basically requires preserving the innate vascular tree, encompassing arteries, veins, and capillaries, during the decellularization process. Thus, creating new vessels with defined ultrastructure and three-dimensional organization and branching is not essential. These intrinsic vascular structures play a crucial role in delivering cells during the recellularization process [168].

Efficient full reendothelialization of the vascular structures within the bioengineered liver is achieved when these structures are covered by a single complete layer of endothelial cells, serving as a non-thrombogenic barrier. This endothelial layer reduces the risk of blood coagulation and protects the hepatocytes from shear stress resulting from blood flow outside the vascular spaces [9,10,108,168]. Several researchers have reseeded the decellularized livers with different types of endothelial cells through the hepatic artery or portal vein in antegrade or retrograde directions, while others have combined both routes. In most cases, these cells remain on the blood vessel surface and line the basal membrane [9–11,14]. For example, Uygun et al. attempted to seed the rat liver scaffold with microvascular endothelial cells into the portal vein 24 h after repopulation by hepatocytes and allowed media perfusion for 5 days [12]. Histological analysis demonstrated the capability of the endothelial cells to cover the blood vasculature. Additionally, Baptista et al. reseeded the ferret liver scaffold with fluorescently labeled ECs through antegrade infusion via the portal vein or retrograde cell infusion through vena cava to investigate the distribution and localization of endothelial cells within the parenchymal and nonparenchymal spaces [13]. Upon reseeding the cells through the portal vein, the cells were observed in the periportal area, whereas when seeded through the vena cava, they were deposited in the pericentral area.

Although injecting ECs into existing blood vessels is a simple technique that relies on the capability of ECs to adhere to the luminal surface of blood vessels, leakage of some ECs outside the vascular structures into the parenchyma, cell detachment under physiological flow conditions, and reendothelization of microvascular structures such as sinusoids remain obstacles to achieving complete reendothelialization of the decellularized liver [14]. Thus, improving reendothelialization efficacy is necessary to prevent platelet adhesion and thrombosis.

4.4.1. Enhancement of the reendothelialization efficiency

Numerous studies have explored different agents to promote EC adhesion and/or enhance cell scaffold interactions to facilitate the attachment, growth, and proliferation of ECs within the decellularized liver. These agents, such as antithrombotic agents, antibodies, growth factors, and/or ECM proteins, exert their effects through various mechanisms, as shown in Figs. 3 and 4 [9–11,14,150,218].

4.4.1.1. Heparin. Heparin, a naturally occurring highly sulfated glycosaminoglycan, is commonly used as an antithrombotic agent. Surface-immobilized heparin has been applied during preparation of different biomaterials to ameliorate the hemocompatibility of coated surfaces by interacting with vascular endothelial growth factor receptors (VEGFRs) on ECs and preventing platelet adhesion [225,226]. Bao et al. were the first to describe heparin immobilization within rat liver scaffold, primarily for reducing coagulation *in vivo* rather than improving reendothelialization efficiency [218]. They pretreated decellularized liver lobes with heparin via the layer-by-layer self-assembly technique, recellularized them with rat hepatocyte spheroids, and implanted them into the portal system in a 90 % hepatectomized rodent model. Transplanted grafts supported hepatic function for 72 h, preserving hepatocyte morphology and prolonging animal survival. Moreover, they applied a similar approach in another study involving clinical-scale porcine liver [219], followed by recellularization with rat primary hepatocytes and HUVECs. They observed that heparin treatments effectively prevented thrombosis in the bioengineered liver during blood perfusion after *in vivo* implantation.

4.4.1.2. Gelatin. Gelatin, a high-molecular-weight natural protein obtained from the hydrolysis of collagen, exhibits excellent biocompatibility and biodegradability [227,228]. Meng et al. perfused endothelial cells in gelatin hydrogel to improve the reendothelialization of decellularized liver scaffolds [108]. They reported a significant increase in the retention of injected endothelial cells within the decellularized liver scaffolds, resulting in a higher vascular lumen perimeter coverage ratio compared to perfusing ECs in Roswell Park Memorial Institute (RPMI) medium. Hussein et al. combined both heparin and gelatin as a mixture to create a sticky surface on blood vessel surfaces, improving reendothelialization efficiency in decellularized porcine liver (Fig. 4) [14]. Livers reendothelialized using EA. hy926 ECs in a dynamic culture in a bioreactor for 10 days showed no clots after *ex vivo* blood perfusion for 24 h. Moreover, they cocultured HepG2 cells and endothelial cells in the decellularized liver and transplanted it heterotopically into pigs, observing no obvious thrombosis and better hepatocyte function compared to uncoated liver scaffolds.

4.4.1.3. Anti-CD31 antibodies. CD31 antibody conjugation on the blood vessels surface of kidneys and livers has been investigated. Ko et al. pretreated decellularized porcine liver scaffold with a CD31 antibody followed by immobilization using N-Hydroxy succinimide (NHS) and 1-ethyl-3-(3- (dimethylamino)propyl)-carbodiimide hydrochloride (EDC) [11]. Then, they infused murine ECs (MS1) into the portal vein, hepatic artery, suprahepatic inferior vena cava, and intrahepatic inferior vena cava. This approach resulted in well-aligned, and uniformly distributed ECs over the lumens of the vascular structures, with a significant reduction in platelet adhesion upon blood perfusion *in vitro* (Fig. 4). Reendothelialized livers sustained physiological host blood flow for up to 24 h after heterotopic transplantation into pigs. Kim et al. coated the decellularized rat liver with anti-CD31 aptamer or anti-CD31 antibodies, then seeded the scaffolds with HUVEC cells and subjected to bioreactor culture for 7 days [9]. Formation of continuous endothelium along the

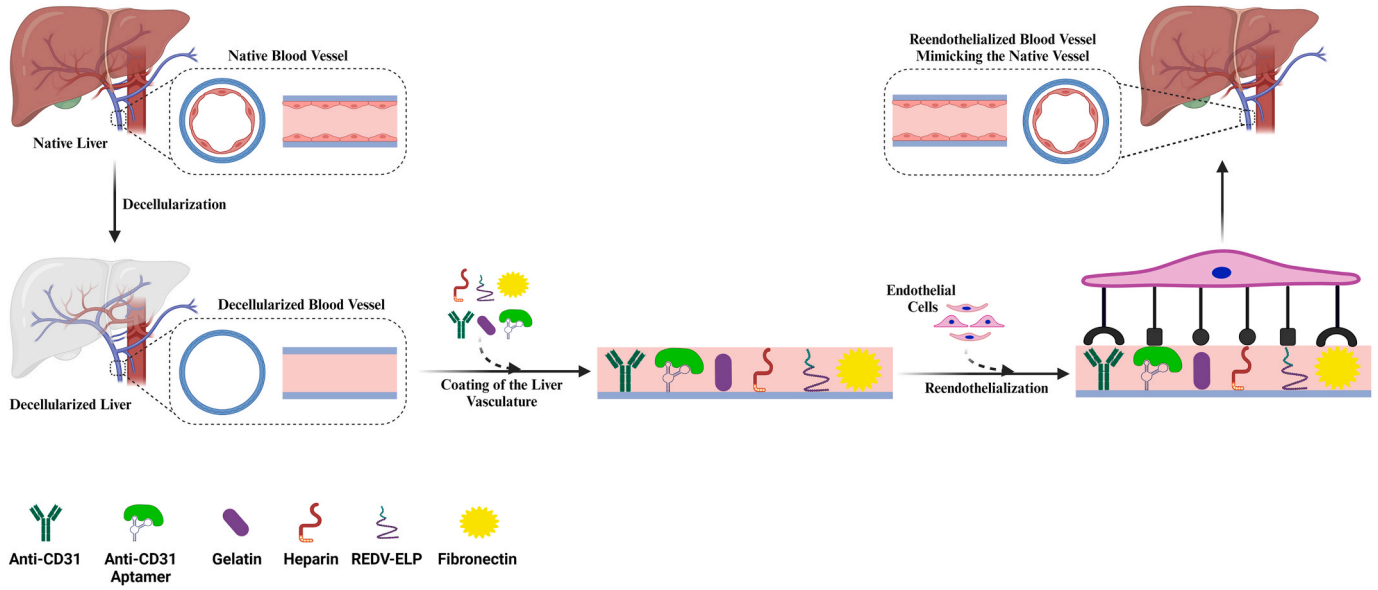

Fig. 3. Mechanism of commonly employed agents to enhance reendothelialization efficiency within the decellularized liver.

vascular lumens was observed in the presence of the anti-CD31 aptamer coating, leading to more efficient endothelization throughout the liver construct than with the anti-CD31 antibody as shown in Fig. 4.

4.4.1.4. REDV conjugated with ELP. Devalliere et al. infused Arg-Glu-Asp-Val (REDV) conjugated with Elastin-like peptide (ELP) that can aggregate to the fusion protein upon thermal triggering, through the portal vein to coat the vasculature within decellularized rat livers for improving endothelial cell attachment [10]. ELP sequences conferred the biopolymer with mechanical properties of native elastin, while REDV enhanced attachment by targeting the adhesion receptor α4 β1 integrin. It is worth to mention that these receptors are found only on the ECs surface, but not on platelets [229]. This specific affinity of REDV peptide for ECs makes it an excellent candidate for enhancing reendothelialization within bioengineered livers. Uygun and her colleagues confirmed this by perfusing decellularized livers with REDV–ELP, showing a significant increase in EC attachment, spreading, and proliferation, with growth of an endothelial monolayer on vascular walls (Fig. 4). Additionally, REDV–ELP conjugation reduced platelet adhesion and activation upon *ex vivo* perfusion with platelet-rich plasma [10].

4.4.1.5. Fibronectin. Fibronectin, a large adhesive glycoprotein, is considered a major component present in decellularized tissues and has been extensively used for conjugation with biomaterial surfaces to accelerate the attachment, spreading, and differentiation of ECs [150,230,231]. Watanabe et al. investigated the ability of fibronectin, combined with flow-derived mechanical stress, to enhance reendothelialization [150]. Decellularized rat livers were treated with fibronectin before HUVECs were introduced into the livers through the portal vein. Perfusion at a rate of 4.7 ml/min was noted to facilitate the generation of sinusoid-scale microvessels, unlike perfusion rates of 2.4 and 9.4 ml/min. Furthermore, the incorporation of fibronectin coating onto decellularized liver scaffolds was found to facilitate the development of sinusoid-scale microvessels during perfusion culture at 4.7 ml/min. However, a limitation of the study by Watanabe et al. is that the authors did not evaluate the hemocompatibility of the vascular networks within the decellularized livers either in an *ex vivo* blood perfusion system or *in vivo*. It is worth mentioning that the use of ECM proteins such as fibronectin has several reported disadvantages. For instance, the use of fibronectin may be associated with a risk of an immune response from the recipient. Additionally, immobilized proteins display high instability and degradability upon exposure to culture medium [232]. Moreover, fibronectin has a high thrombogenic potential and can initiate the coagulation cascade when the biomaterial coated by fibronectin comes in contact with the patient's blood *in vivo* [233].

4.4.1.6. Other agents. Other agents, including fucoidan (FU), laminin, hyaluronic acid (HA), chondroitin sulfate, type 1 collagen, and vascular endothelial growth factor (VEGF), have been used to improve endothelialization on the surface of nano and metal stents as well as thin tissues such as heart valve and blood vessels [231,234]. These agents can interact with ECs to induce adhesion and with platelets to decrease the risk of thrombosis, potentially enhancing reendothelialization within decellularized livers. Further investigation is needed to assess the efficacy of these agents in improving reendothelialization efficiency in decellularized liver scaffolds.

4.4.2. Cell sources

As a prerequisite, cells used for vascular reconstruction should be non-immunogenic, able to proliferate to produce a high number, easily harvested, and retain the function of the endothelial cells as in native vessels.

4.4.2.1. Adult ECs. Endothelial cells are of significant interest in tissue engineering and regenerative medicine. However, their application is limited due to the donor variability, technical challenges of isolation, limited proliferative capacity, senescence, and heterogeneity [235,236]. Cell lines, including HUVECs and EA. hy926 cells, have been extensively used for reendothelization of decellularized livers due to their relative ease of accessibility and the non-invasive harvesting from medical waste, in addition to a high yield following isolation [10,13,14,235]. Both cell types were able to line the blood vessels of decellularized livers, with a significant reduction in platelet adhesion and clot formation during *ex vivo* blood perfusion and demonstrated the ability to withstand blood flow after *in vivo* transplantation in pigs. The main disadvantages are their immunogenicity and the difficulty of using as autologous endothelial cell source. Additionally, HUVECs have exhibited poor engraftment, limited capacity to form vessels, and an inability to survive long-term after *in vivo* application [237,238].

4.4.2.2. Endothelial progenitor cells. Endothelial progenitor cells (EPCs) are circulating cells in peripheral blood originating from the bone

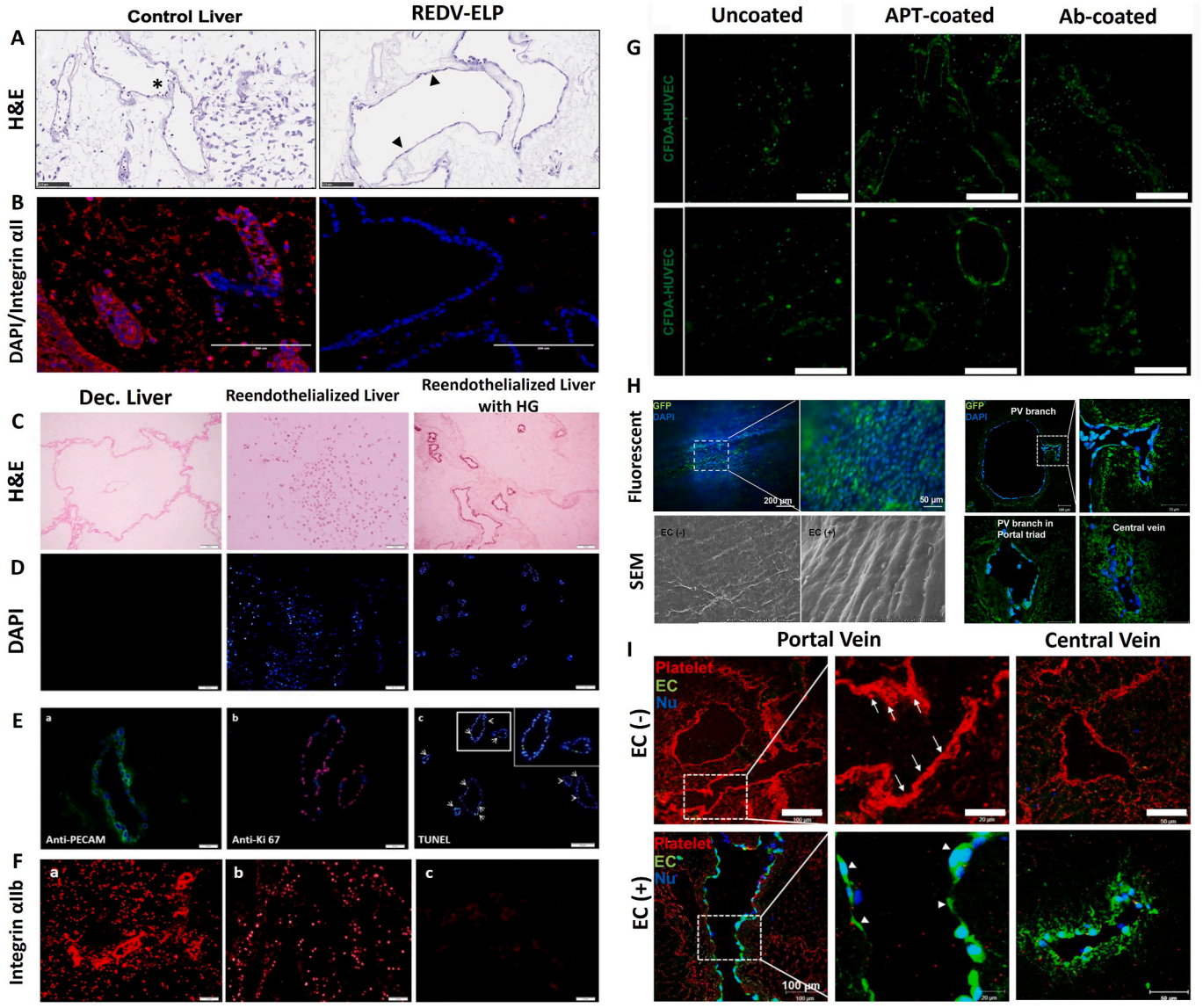

Fig. 4. Improving the reendothelization efficiency in decellularized liver scaffolds. (A) Hematoxylin and eosin (H&E) staining of decellularized rat liver scaffolds after reseeding with human EA. hy926 endothelial cells with 4 days of perfusion. In the control liver, cells were partially detached from the vessel wall or accumulated inside vessel lumens (asterisk), whereas a monolayer of well-spread endothelial cells (arrowhead) was observed covering the vessel walls after coating by REDV-ELP (Scale bar = 100 μm). (B) Immunostaining of reendothelialized scaffolds with anti-integrin αIIb antibodies (shown in red) and DAPI (shown in blue), confirming the presence of a limited number of platelets on vasculature of the REDV-ELP reendothelialized scaffolds. In contrast, high levels of platelet were detected within the control liver scaffold. Scale bar: 200 μm [Adapted from Devalliere et al. [10] with permission from Elsevier]. (C, D) H&E and DAPI staining revealed an absence of cells in decellularized liver. ECs were observed in the parenchyma in the uncoated scaffolds, while cells were located on the vasculature in the heparin gelatin-coated scaffolds. Scale bar = 10 μm. (E) Anti-PECAM staining confirmed the presence of ECs as a monolayer on the vessel lumen (a), with the ability to proliferate as shown by Ki-67 staining (b). Few numbers of cells were apoptotic as revealed by TUNEL assay (c) (White arrow indicates the apoptotic cells). (F) Anti-integrin αIIb immunostaining showed a significant platelet adhesion and aggregation inside and around the vasculature (a) after blood perfusion. The reendothelialized scaffolds without heparin-gelatin coating exhibited a significantly higher positive signal (b) compared to that of heparin-gelatin-precoated scaffolds (c). Scale bar = 10 μm [Adapted from Hussein et al. [14], with a permission from Elsevier]. (G) Immunofluorescence staining of reendothelialized rat liver scaffolds with CFDA-labeled HUVECs without the coating agent (Uncoated), or with the following coating agents; anti-CD31 aptamer (APT-coated) and anti-CD31 antibody (Ab-coated) after 7 days. Magnified images were shown (bottom). Scale bar for the top images: 200 μm, and for the bottom: 100 μm [Adapted from Kim et al. [9], with a permission from Elsevier]. (H) Uniform and properly aligned reendothelialization of the PV of the decellularized porcine liver was confirmed by GFP expression and SEM analysis on attached murine endothelial cells (MS1), respectively. (I) *Ex vivo* blood perfusion of scaffolds led to a significant platelet adhesion (aIIb positive staining) on blood vessels of the unseeded scaffold, as indicated by arrows, while platelet attachment (arrowheads) was significantly reduced in the reendothelized scaffolds conjugated with CD31 antibodies [Adapted from Ko et al. [11], with a permission from Elsevier].

marrow, representing approximately 0.01 % of all blood mononuclear cells, with some cells residing in the adipose tissue of adults [234]. This results in the easy isolation of autologous EPCs from peripheral blood, lipoaspirate tissue, and bone marrow in sufficient number, holding promising potential for reendothelization of decellularized livers for clinical application [239]. Furthermore, EPCs have been reported to have a higher angiogenic potential than ECs [240]. Zhou et al. infused decellularized rat livers through the portal vein with EPCs isolated from rat bone marrow. The reseeded cells covered the vascular structures within the decellularized liver after 3 days of media perfusion [105].

Lack of standardized criteria for characterizing and identifying EPCs, age of donors and their clinical conditions, and ethnicity of populations

may negatively affect the viability and function of EPCs [241].

4.4.2.3. Induced pluripotent stem cells. iPSC-ECs have been produced from different cell sources by multiple methods with superior proliferative capacity [236]. Human iPSC-derived ECs can form blood vessels and anastomose with the host vasculature when injected into a zebrafish model [238]. Takeishi et al. differentiated human iPSC into iPSCs-derived vascular ECs and reseeded the differentiated cells into rat decellularized liver [242]. The cells engrafted in the scaffold's vascular structure and showed enhanced expression of angiogenesis and anticoagulation-related genes and functions in the organ-like environment.

4.5. Biliary tract reconstruction

One of the challenges that need to be addressed is reconstructing a functional biliary tree within the bioengineered liver. Daily, the healthy human liver produces about 750 ml of bile to aid in the digestion of lipids, with hepatocytes being the main contributors to its secretion, passed to the gall bladder through the bile ducts [243].

Cholangiocytes are the epithelial cells that line the intra- and extrahepatic ducts of the biliary tree and participate in the formation, modification, and transportation of bile through their transmembrane molecules. Although these cells represent only approximately 3 %–5 % of the total liver cell population, they are necessary for maintaining different normal physiologic processes. Furthermore, cholangiocytes act as an active barrier between the cytotoxic bile and surrounding tissue [244]. Thus, rebuilding the intrahepatic as well as extrahepatic biliary ducts of the biliary network within the bioengineered liver is crucial to construct a fully functional liver organ and avoid severe liver damage as a post-transplant complication. Fortunately, the biliary network tree is confirmed to be intact after decellularization by scan electron microscopy, corrosion cast, dye perfusion, and contrast radiography; only reconstruction by bile duct cells is necessary [12,110,170,198].

Although several studies have reported the recellularization of the decellularized liver with hepatocytes, there have been very few trials for repopulating the biliary tree with cholangiocytes. This may be attributed to the difficulty of isolating cholangiocytes in sufficient numbers, their de-differentiation after a few passages, loss of function and phenotype during propagation, as well as the tortuous and complex architecture of the biliary network [111,245–247].

4.5.1. Cell sources

4.5.1.1. Primary cholangiocytes. Chen et al. recellularized the decellularized rat liver by infusing primary cholangiocytes through the bile duct and hepatocytes through the portal vein [111]. Importantly, they reported that the biliary tree within the decellularized liver scaffold remains almost impermeable and closed at the ends of the smallest ductules, allowing the retention of any liquid injected into the extrahepatic bile duct without diffusion into the parenchyma. Therefore, they injected the cholangiocytes in a volume only sufficient to fill the bile ducts, followed by a 1-h static culture to allow the attachment of the cholangiocytes to the bile ducts. After 48 h of dynamic perfusion, they observed that the biliary epithelial cells formed duct-like structures, with the viable hepatocyte mass residing in the parenchymal space, in an arrangement mimicking the native tissue. Interestingly, compared to decellularized livers reseeded by hepatocytes only, scaffolds recellularized with both cholangiocytes and hepatocytes revealed slightly higher levels of cumulative albumin production and urea secretion.

4.5.1.2. Fetal liver hepatoblasts. Fetal liver hepatoblasts have been used as a surrogate for primary cholangiocytes. Baptista et al. demonstrated the capacity of decellularized livers to induce the differentiation of fetal hepatoblasts into biliary and hepatocytic lineages [13]. Additionally, Ogiso et al. showed the presence of organ-specific cell–ECM communication that enhanced the maturation of reseeded fetal hepatocytes within decellularized rat livers into both hepatocyte and cholangiocyte lineages, without the addition of any pro-differentiation signals into the culture media during 7 days of dynamic perfusion [217].

4.5.1.3. Organoids. Recently, organoid technology has shown great promise for regenerative medicine due to its ability to differentiate, self-organize, and proliferate in high and stable capacity without losing the desirable cholangiocyte phenotype [248,249]. This makes the organoids an attractive cell source for biliary tree reconstruction. In 2015, Huch et al. were the first to describe the establishment of cholangiocyte organoids from human liver biopsies [250]. They employed EpCAM to sort hepatocytes (EpCAM-) from ductal EpCAM + ductal cells and reported that these EpCAM + cells developed into organoids with an efficiency of 28.4 %. The developing organoids displayed a duct-like phenotype, expressing both cholangiocyte markers (KRT 7 and KRT 19) and progenitor stem cell markers (Sox 9 and LGR-5) with high proliferative capacity. Following this study, successful production of organoids from extrahepatic bile duct, gall bladder, and bile has been demonstrated [251–253]. These organoids exhibited transcriptomic and phenotypic differences between cholangiocytes of different origin within the biliary tree [254].

Tomofuji et al. reconstructed intrahepatic bile ducts in a rat decellularized liver by reseeding with liver ductal organoids [255]. Upon *ex vivo* culture perfusion for 3–5 days, the repopulated organoids engrafted along the bile duct walls, reconstructed biliary tree-like networks with luminal structures, and expressed cholangiocyte marker genes (Fig. 5), including KRT 19, Sox 9, CFTR, and Hnf1b, and sustained the expression of stemness markers (Lgr5, Prom 1).

Willemse et al. recellularized discarded decellularized human extrahepatic bile ducts with cholangiocyte organoids obtained from different origins including liver biopsies, extrahepatic bile duct biopsies, and bile samples [256]. Compared to organoids of intra hepatic origin, extra hepatic and bile-derived organoids demonstrated more efficient repopulation of the decellularized duct. After 7–10 days of recellularization of the bile duct disc, a transparent rim was seen surrounding the edge of the decellularized duct in extrahepatic and bile-derived organoid-recellularized samples. This rim was not clear and did not cover the entire disc in the case of intra hepatic organoid-recellularized ducts. Additionally, extrahepatic and bile-derived organoids displayed profound tight junctions and polarity with apical cilia, with expression of mature cholangiocyte markers and increased electrical resistance, suggesting the restoration of the barrier function. At the end of the 21-day period, the decellularized human extrahepatic bile duct scaffolds exhibited full luminal surface coverage with a confluent monolayer of cholangiocyte-like cells following reseeding. Repopulated cells expressed different mature cholangiocyte markers including KRT 7, KRT 19, CFTR, and SCTR.

Collectively, these studies provided evidence that intrahepatic origin, extrahepatic and bile-derived organoids can efficiently repopulate the decellularized bile duct while retaining the gene expression profile that closely resembles primary cholangiocytes *in vivo*.

5. Transplantation models

In vitro evaluations and *ex vivo* blood perfusion systems enable the researchers to investigate the function of reseeded hepatic cells and cholangiocytes, as well as the integrity of the endothelial lining of liver scaffolds. However, *in vivo* transplantation studies are critical at a regulatory level for evaluating the aforementioned parameters in addition to potential inflammatory and/or immune responses, and importantly, the applicability of bioengineered livers toward clinical applications. Preserved vascular structures after liver decellularization allow for the opportunity to transplant the bioengineered liver either heterotopically

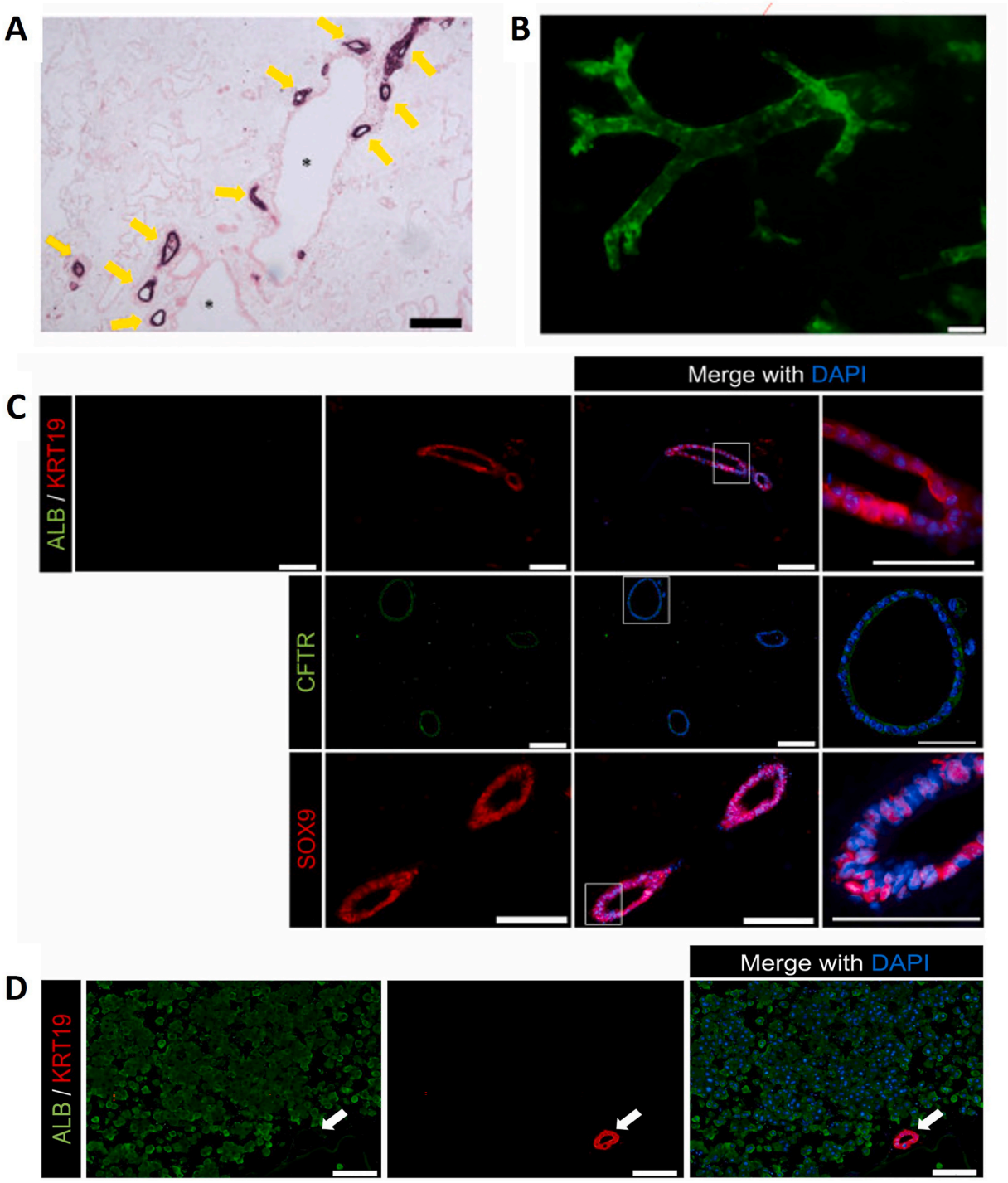

Fig. 5. Biliary reconstruction in decellularized mouse liver. (A) H&E staining of the liver scaffold, showing engrafted bile ducts after reseeding with mouse liver ductal organoids (yellow arrows). Scale bars: 200 μm. (B) Fluorescent microscopic examination of bile ducts recellularized with liver ductal organoids expressing GFP on day 5 of perfusion culture (Scale bar: 250 μm). (C) Immunofluorescence images of reseeded bile ducts stained with albumin and KRT 19, Sox 9, and CFTR. Scale bars: 100 μm. Higher magnification images of the outlined boxed areas are presented in the right panels (scale bars in high-magnification images: 50 μm). (D) Immunofluorescence staining of the liver scaffold sections against albumin and KRT19, demonstrates the appropriate cell distribution, with liver ductal organoids located within the bile duct and primary hepatocytes found within the parenchyma. White arrows indicate bile ducts (Scale bars:100 μm). [Adapted from Tomofuji et al. with permission from Elsevier [255]].

or orthotopically in mice, rats, and pigs by connecting the graft to the recipient blood vessels. Commonly, the portal vein and infrahepatic IVC in the liver scaffold are connected to the aorta and IVC or renal artery and renal vein, respectively [11,12,14].

5.1. Rodent models

Rodents are valuable for evaluating the survival and function of reseeded cells, thrombogenicity, and immunogenicity of the bio-engineered liver, and are preferred over large animals as they are easy to breed, maintain, less costly, and ethically acceptable [257]. Over the last

decade, several groups reported the implantation of ferret, mice, and rat decellularized livers after recellularization with hepatocytes with/-without endothelial cells into allogenic rodent as reported in Table 1 [9,12,13,108,218]. Uygun et al. impanated the decellularized rat liver reseeded with primary rat hepatocytes [12]. They performed unilateral nephrectomy and anastomosed the graft portal vein and hepatic artery to the recipient renal artery and renal vein, respectively, for 8 h. The reseeded cells within the scaffold were able to retain function, normal morphology, and location within the parenchyma of the scaffold.

Induction of acute or chronic liver failure prior to transplantation of the scaffold is another important step toward understanding the full function of the bioengineered liver. Bao et al. decellularized the rat liver, performed layer-by-layer heparin deposition, and repopulated the scaffold with hepatocytes [218]. They transplanted the scaffold into the portal systems of 90 % hepatectomized rats for 72 h. The transplanted scaffold improved liver function, decreased blood ammonia levels, and prolonged survival compared to a 90 % hepatectomy.

Kim et al. transplanted bioengineered rat livers fabricated with the

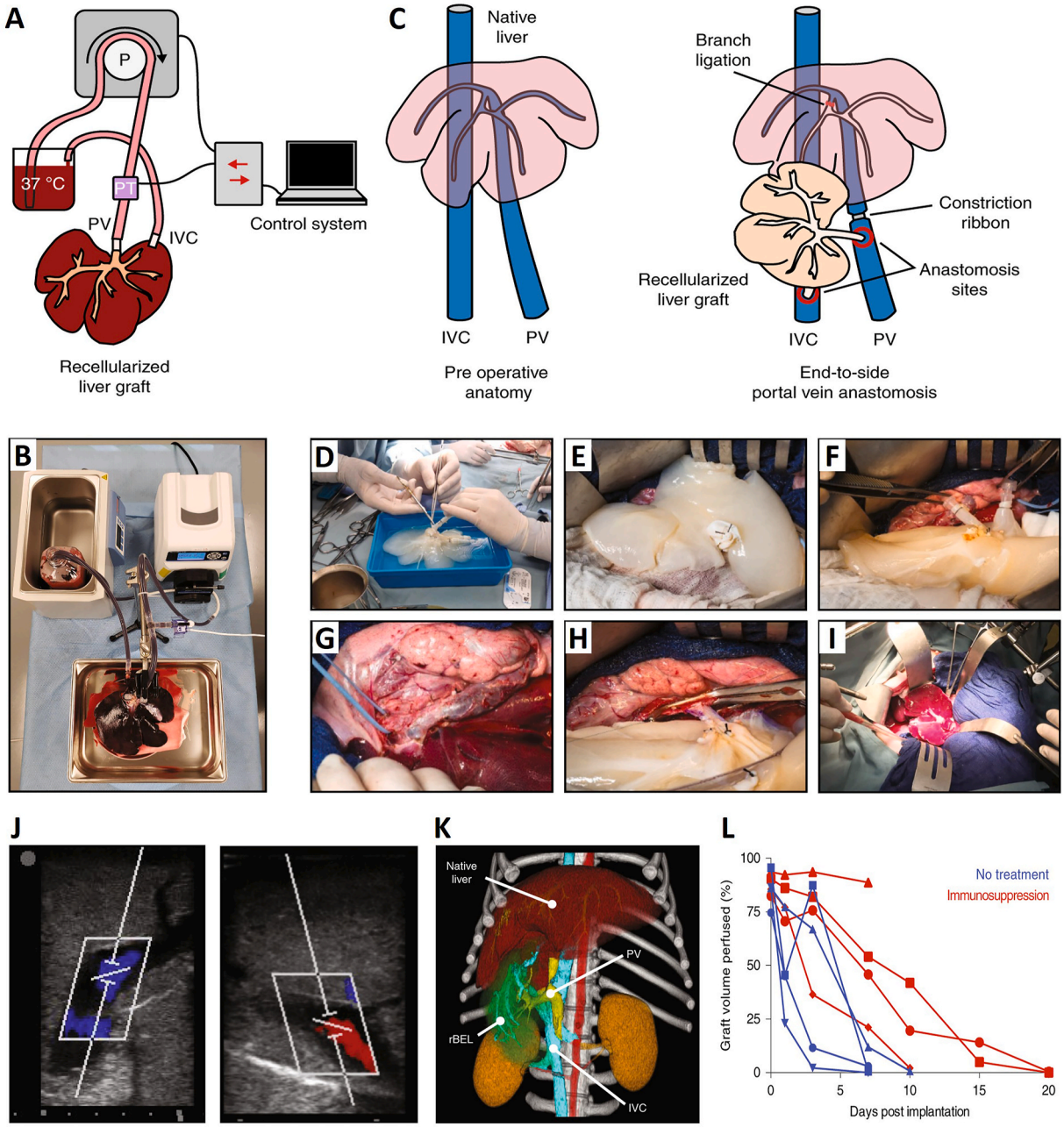

Fig. 6. *In vivo* transplantation of bioengineered livers in a porcine model. (A, B) Depiction of the *in vitro* blood circuit setup used to investigate the vascular patency of the reendothelized liver. (C) A diagram of an *in vivo* heterotopic liver transplantation model, wherein the liver scaffold is connected via the PV and IVC to the recipient's PV and IVC. (D–I) Representative images of the heterotopic liver implant process, including reendothelized liver scaffold preparation (D), positioning in the abdominal cavity (E), positioning of scaffold vessels prior to anastomosis (F), constriction of the native PV (G), anastomosis of scaffold vessels with native PV and IVC (H), and scaffold reperfusion (I). (J) Representative ultrasound images of an implanted reendothelized liver scaffold showing portal (left) and hepatic (right) venous flow after 30 min. (K) Three-dimensional computed tomography (CT) reconstruction after graft transplantation, demonstrating the heterotopic position of the implanted liver graft below the native liver while showing good vascular perfusion of the implanted graft. (L) Quantification of graft perfusion reduction over time in untreated and immunosuppressed pigs. Each symbol represents an independent liver scaffold implant. [Adapted from the study by Shaheen et al. with permission of Nature Biomedical Engineering, copyright 2020 [8]].

nano-graphene oxide cross-linking into liver failure mouse models induced by 70 % partial hepatectomy and thioacetamide, respectively [178]. This model enabled the authors to validate the *in vivo* regenerative capacity of the scaffolds. The disadvantages of rodents as a model are the insufficient abdominal space that impedes the transplantation of the whole liver. Thus, these studies performed transplantation of only one or few lobes after unilateral nephrectomy. Additionally, although a rodent model could give initial expectations about cell function within the transplanted liver, vascular patency, and graft immunogenicity, findings from such animal models often do not translate into human clinical applications due to size and anatomical differences.

5.2. Large animal models

In general, pigs are preferred as their livers resemble human livers in many ways, including size, anatomy, and physiology. Thus, through this model, the function, potential thrombogenicity, and immune response of the bioengineered liver, and the scaffold's ability to withstand the shear stress created by normal portal venous flow and pressure, along with surgical complications, can be evaluated in a more realistic approach. Unilateral nephrectomy provides space for transplanting one lobe or the whole bioengineered liver. Since different researchers used human cells for recellularization or reendothelization of the scaffold, administration of immunosuppressants is required [192]. Barakat et al. performed auxiliary transplantation of the porcine decellularized right lateral lobe into a recipient pig, immunosuppressed with methylprednisolone [23]. The bioengineered liver lobe was implanted in the infrahepatic space using the recipient portal vein and infrahepatic inferior vena cava as an inflow and outflow, respectively, and reported to maintain the integrity of the scaffold during 2 h of transplantation. Hussein et al. reendothelialized the decellularized porcine right lateral liver lobe with EA. hy926 endothelial cells after coating the vasculature using heparin-gelatin mixture, then the lobe was reseeded with HepG2 cells [14]. They transplanted the bioengineered lobe heterotopically in a pig for 1 h and reported that the patency of the vascular tree upon contrast radiography with down-regulated expression of the coagulation markers and a higher expression of the hepatic liver function in heparin-gelatin precoated liver scaffolds. This study indicated the efficiency of the heparin gelatin coating in improving the efficiency of reendothelialization and maintaining the function of the parenchymal cells *in vivo*.

Our group induced immunosuppression in recipient pigs by splenectomy and methylprednisolone administration before transplanting the decellularized liver reendothelialized with HUVECs as shown in Fig. 6 [8]. We observed that immunosuppression led to a significant reduction in immune responses and resulted in longer graft perfusion and vascular patency of the graft for over 14 days compared to the group without immunosuppression. Interestingly, with immunosuppression withdrawal, graft thrombosis occurred similar to non-immunosuppressed group, indicating that xenogeneic immune response against HUVECs played a critical role in thrombosis and graft loss. To go further, in another study, we successfully reseeded a decellularized liver scaffold, previously reendothelialized with HUVECs, with primary porcine hepatocytes [193]. We devascularized the native liver *in situ* by ligating the native portal vein and hepatic artery. Then, the bioengineered livers were implanted in the auxiliary position caudal to the native liver. Repopulated hepatocytes within the bioengineered liver were functional and able to produce albumin, detoxify ammonia, and synthesize urea for up to 48 h.

Higashi et al. reseeded the right lateral lobe of the decellularized liver with primary hepatocytes and endothelial cells [258]. Immunosuppression of recipient pigs was induced through splenectomy as well as immunosuppressant drugs, including ticlopidine, prednisolone, and tacrolimus during postoperative period. Then, the scaffold was transplanted in pigs with 60 % hepatectomy as induced liver failure model for 28 days. Importantly, the animals received aspirin and ticlopidine to prevent platelet aggregation in addition to heparin as an anticoagulant. The bioengineered scaffold showed good repopulation of the hepatocytes graft with improved liver function and exhibited upregulation of liver-specific genes. This study is noteworthy as the first to document a 28-day post-transplant analysis of a bioengineered liver graft in a preclinical large animal model.

6. Regulatory measures

As of yet, there are no specific FDA guidelines exclusively addressing the use of bioengineered liver organs that are produced through combined decellularization and recellularization approaches. The regulation involving the use of recellularized tissues would be similar to those associated with decellularized tissues, with some additional factors specific to the reintroduction of cells. Generally, the use of those bioengineered livers would subject to broader FDA regulations related to medical devices, biologics, and human cells, tissues, and cellular and tissue-based products (HCT/P) [259].

First, informed consent and ethical considerations for using human/animals' livers as well as the use of human cells for recellularization must be addressed in accordance with regulatory guidelines. Second, manufacturing of decellularized organs must comply with Good Manufacturing Practice regulations (GMP) to ensure the quality, safety, consistency, and effectiveness of the tissue after decellularization. Setting acceptable limits for toxic decellularizing agents within decellularized liver scaffolds is critical in compliance with FDA regulations. While achieving absolute sterility may not be feasible due to the presence of living cells, stringent quality control measures, including the assessment and regulation of residual contaminants, are essential to ensure the safety and efficacy of decellularized liver intended for recellularization and subsequent clinical application. Third, reseeding the decellularized organ introduces additional complexity and safety considerations. Thus, regulatory agencies would require detailed information on the cell source, including donor screening to prevent the transmission of infectious diseases, complete cell characterization, validation of the recellularization procedure, and evidence of cell viability and functionality within the recellularized organ. Assessments of both immunogenicity and compatibility between the reseeded cells and the decellularized ECM are important for regulatory approval to ensure proper integration of cells. Fourth, preclinical and clinical trials are essential to provide additional evidence of safety and effectiveness.

7. Conclusion and future perspectives

Liver tissue engineering is rapidly evolving with the ambitious aim of revolutionizing the field of hepatology and liver transplantation. Recently, three-dimensional bioprinting has emerged as a promising technology for constructing tissues and organs, for both drug screening and potential transplantations. Barranger et al. utilized CometChip technology to construct a 3D model of HepaRG human liver cells, facilitating toxicology and disease studies [260]. Similarly, Vernetti et al. pioneered a self-assembly liver model for physiological, drug safety, and disease investigations [261]. Moreover, various studies have explored the use of decellularized liver bioink alone or in combination with other materials for 3D bioprinting of liver constructs [262,263]. This technology exhibits substantial potential due to its precise control and its ability to uniformly distribute cells across a complex structure. However, the application of liver bioprinting for transplantable whole functional liver organs is still in its infancy and requires extensive further development and expansion. This review focused on liver graft production by decellularization and recellularization especially mammalian liver (human, pig) because of superior scalability of this method and its potential for clinical application.

Over the past 14 years, since Uygun et al. pioneered liver decellularization and recellularization, significant progress has been made in perfusion decellularization/recellularization technology [12]. This

progress has enabled the creation of clinically relevant decellularized/recellularized liver scaffolds with intact vascular linings, holding promise for regenerative medicine. Despite these advancements, transitioning bioengineered liver scaffolds to clinical transplantation trials faces several challenges, necessitating further investigation and development. Additionally, these bioengineered livers can serve as scaffolds for developing devices capable of temporarily supporting liver function in patients with liver failure. For instance, the clinical trial "A Phase 1 prospective study of the Miromatrix external liver assist product (miroliverELAP®) for liver support in adults with acute liver failure" (ClinicalTrials.gov Identifier: NCT06285253) [264] is currently investigating the efficacy of the miroliverELAP® system, an *ex vivo* supported bioartificial liver system, in treating acute liver failure.

Immunogenicity of the decellularized liver scaffolds remains a primary concern, particularly due to limited studies in large animal models without immunosuppression. The use of immunosuppressive drugs, combined with the lack of *in vivo* long-term evaluation of the bioengineered liver, has led to unrealistic investigations of ECM immunogenicity. Nevertheless, the approval of a wide range of decellularized tissue scaffolds from various sources such as human dermis and pulmonary valve, porcine small intestine, urinary bladder, and dermis, and bovine pericardium products by the FDA for clinical use suggests progress in overcoming immune-related issues [265]. The clinical approval of these scaffolds highlights the safety, efficacy, and biocompatibility of these decellularized tissues in supporting tissue regeneration in humans, addressing concerns about potential immune reactions of decellularized ECM. Decellularization protocols vary between labs, resulting in different constituents within livers produced by different protocols. Therefore, standardization of decellularization techniques and quality assessment, including biocompatibility testing, to ensure absence of any cytotoxic agents within the scaffolds as well as depletion of both xenogeneic and pathogenic epitopes for addressing potential host immune responses and zoonotic concerns, respectively, are another challenge necessary to meet both experimental and clinical application standards.

Repopulating the parenchymal region in decellularized scaffolds with functional hepatocytes is crucial. Different techniques and cell types have been employed for reseeding the liver scaffolds. The use of primary hepatocytes has shown reproducibility but has only yielded initial signs of significant function, such as temporary stabilization of serum ammonia in one of our *in vivo* studies [193]. MSCs and iPSCs hold significant promise for clinical applications due to their unique properties and potential therapeutic benefits.

Challenges also persist in reconstructing a complete and functional endothelial cell layer, necessitating strategies for micro-capillary reconstruction and uniform endothelial cell coverage. Finally, the reconstruction of the biliary system and the redistribution of various cell types remain unaddressed, highlighting the complexity of achieving fully functional liver substitutes.

Future efforts must also address logistical challenges such as organ availability, instrumentation requirements, cost considerations, and regulatory approvals to facilitate broader clinical translation. Collaborative research efforts hold promise for revolutionizing liver regeneration and transplantation, offering hope to patients in need of life-saving interventions.

Ethics approval and consent to participate

Not applicable.

CRediT authorship contribution statement

Kamal H. Hussein: Writing – review & editing, Writing – original draft, Visualization, Validation, Methodology, Investigation, Data curation, Conceptualization. **Boyukkhanim Ahmadzada:** Writing – review & editing. **Julio Cisneros Correa:** Writing – review & editing. **Ahmer Sultan:** Writing – review & editing. **Silvana Wilken:** Writing – review & editing. **Bruce Amiot:** Writing – review & editing. **Scott L. Nyberg:** Writing – review & editing, Visualization, Validation, Supervision, Project administration, Funding acquisition.

Declaration of competing interest

The authors certify that they have no affiliations with or involvement in any organization or entity with any financial interest in the subject matter or materials discussed in this manuscript. Figs. 1–3 were created with BioRender software (https://biorender.com/).

Acknowledgements

K.H.H acknowledges support from the Fulbright Visiting Scholar Program (2023–2024).

References

[1] H. Devarbhavi, et al., Global burden of liver disease: 2023 update, J. Hepatol. 79 (2) (2023) 516–537.
[2] C. Ma, et al., Trends in the economic burden of chronic liver diseases and cirrhosis in the United States: 1996–2016, Official J. Am. Coll. Gastroenterol. 116 (10) (2021) 2060–2067.
[3] A.J. Kwong, et al., OPTN/SRTR 2020 annual data Report: liver, Am. J. Transplant. 22 (2022) 204–309.
[4] R. Langer, J.P. Vacanti, Tissue engineering, Science 260 (5110) (1993) 920–926.
[5] K.H. Hussein, et al., Biocompatibility evaluation of tissue-engineered decellularized scaffolds for biomedical application, Mater. Sci. Eng. C 67 (2016) 766–778.
[6] S.F. Badylak, D.O. Freytes, T.W. Gilbert, Extracellular matrix as a biological scaffold material: structure and function, Acta Biomater. 5 (1) (2009) 1–13.
[7] P.M. Crapo, T.W. Gilbert, S.F. Badylak, An overview of tissue and whole organ decellularization processes, Biomaterials 32 (12) (2011) 3233–3243.
[8] M.F. Shaheen, et al., Sustained perfusion of revascularized bioengineered livers heterotopically transplanted into immunosuppressed pigs, Nat. Biomed. Eng. 4 (4) (2020) 437–445.
[9] D.-H. Kim, et al., Development of highly functional bioengineered human liver with perfusable vasculature, Biomaterials 265 (2021) 120417.
[10] J. Devalliere, et al., Improving functional re-endothelialization of acellular liver scaffold using REDV cell-binding domain, Acta Biomater. 78 (2018) 151–164.
[11] I.K. Ko, et al., Bioengineered transplantable porcine livers with re-endothelialized vasculature, Biomaterials 40 (2015) 72–79.
[12] B.E. Uygun, et al., Organ reengineering through development of a transplantable recellularized liver graft using decellularized liver matrix, Nat. Med. 16 (7) (2010) 814–820.
[13] P.M. Baptista, et al., The use of whole organ decellularization for the generation of a vascularized liver organoid, Hepatology 53 (2) (2011) 604–617.
[14] K.H. Hussein, et al., Heparin-gelatin mixture improves vascular reconstruction efficiency and hepatic function in bioengineered livers, Acta Biomater. 38 (2016) 82–93.
[15] G. Mazza, et al., Decellularized human liver as a natural 3D-scaffold for liver bioengineering and transplantation, Sci. Rep. 5 (1) (2015) 13079.
[16] F. Nobakht Lahrood, et al., Generation of transplantable three-dimensional hepatic-Patch to improve the functionality of hepatic cells in vitro and in vivo, Stem Cell. Dev. 29 (5) (2020) 301–313.
[17] W.L. Septiana, et al., Liver organoids cocultured on decellularized native liver scaffolds as a bridging therapy improves survival from liver failure in rabbits, In Vitro Cell. Dev. Biol. Anim. 59 (10) (2023) 747–763.
[18] K.H. Hussein, et al., Decellularized hepatic extracellular matrix hydrogel attenuates hepatic stellate cell activation and liver fibrosis, Mater. Sci. Eng. C 116 (2020) 111160.
[19] F. Panahi, et al., Analysis of decellularized mouse liver fragment and its recellularization with human endometrial mesenchymal cells as a candidate for clinical usage, Prog Biomater 11 (4) (2022) 409–420.
[20] H. Ijima, et al., Decellularized mouse liver as a small-scale scaffold for the creation of a Miniaturized human liver, J. Chem. Eng. Jpn. 56 (1) (2023) 2204899.
[21] T. Shupe, et al., Method for the decellularization of intact rat liver, Organogenesis 6 (2) (2010) 134–136.
[22] H. Ren, et al., Evaluation of two decellularization methods in the development of a whole-organ decellularized rat liver scaffold, Liver Int. 33 (3) (2013) 448–458.
[23] O. Barakat, et al., Use of decellularized porcine liver for engineering humanized liver organ, J. Surg. Res. 173 (1) (2012) e11–e25.
[24] Q. Wu, et al., Optimizing perfusion-decellularization methods of porcine livers for clinical-scale whole-organ bioengineering, BioMed Res. Int. 2015 (2015) 785474.
[25] M.M.A. Verstegen, et al., Decellularization of whole human liver grafts using controlled perfusion for transplantable organ Bioscaffolds, Stem Cell. Dev. 26 (18) (2017) 1304–1315.

[26] J. Willemse, et al., Fast, robust and effective decellularization of whole human livers using mild detergents and pressure controlled perfusion, Mater. Sci. Eng., C 108 (2020) 110200.
[27] A.M. Kajbafzadeh, et al., Determining the optimal decellularization and sterilization protocol for preparing a tissue scaffold of a human-sized liver tissue, Tissue Eng. C Methods 19 (8) (2013) 642–651.
[28] A.K. Israni, et al., OPTN/SRTR 2016 annual data report: deceased organ donation, Am. J. Transplant. 18 (2018) 434–463.
[29] A.J. Kwong, et al., OPTN/SRTR 2021 annual data report: liver, Am. J. Transplant. 23 (2 Suppl 1) (2023) S178–s263.
[30] A. Acun, et al., Liver donor age affects hepatocyte function through age-dependent changes in decellularized liver matrix, Biomaterials 270 (2021) 120689.
[31] P. Rolewska, et al., Age-related expression, enzymatic solubility and modification with advanced glycation end-products of fibrillar collagens in mouse lung, Exp. Gerontol. 48 (1) (2013) 29–37.
[32] S.L. Wilson, et al., A microscopic and macroscopic study of aging collagen on its molecular structure, mechanical properties, and cellular response, Faseb. J. 28 (1) (2014) 14–25.
[33] L.K. Wood, et al., Intrinsic stiffness of extracellular matrix increases with age in skeletal muscles of mice, J. Appl. Physiol. 117 (4) (2014) 363–369.
[34] J.G. Snedeker, A. Gautieri, The role of collagen crosslinks in ageing and diabetes - the good, the bad, and the ugly, Muscles Ligaments Tendons J 4 (3) (2014) 303–308.
[35] P.L. Lewis, et al., Complex bile duct network formation within liver decellularized extracellular matrix hydrogels, Sci. Rep. 8 (1) (2018) 12220.
[36] C. Williams, K. Sullivan, L.D. Black 3rd, Partially digested adult cardiac extracellular matrix promotes cardiomyocyte proliferation in vitro, Adv. Healthcare Mater. 4 (10) (2015) 1545–1554.
[37] S. Tottey, et al., The effect of source animal age upon extracellular matrix scaffold properties, Biomaterials 32 (1) (2011) 128–136.
[38] J. Willemse, et al., Design by nature: emerging applications of native liver extracellular matrix for cholangiocyte organoid-based regenerative medicine, Bioengineering 9 (3) (2022).
[39] E. Lada, et al., Porcine liver anatomy applied to biomedicine, J. Surg. Res. 250 (2020) 70–79.
[40] C. Perleberg, A. Kind, A. Schnieke, Genetically engineered pigs as models for human disease, Dis Model Mech 11 (1) (2018).
[41] A. Heinemann, et al., Standard liver volume in the Caucasian population, Liver Transplant. Surg. 5 (5) (1999) 366–368.
[42] H. Bismuth, Surgical anatomy and anatomical surgery of the liver, World J. Surg. 6 (1) (1982) 3–9.
[43] F.G. Court, et al., Segmental nature of the porcine liver and its potential as a model for experimental partial hepatectomy, Br. J. Surg. 90 (4) (2003) 440–444.
[44] G.A. Sebben, et al., Variations of hepatic artery: anatomical study on cadavers, Rev. Col. Bras. Cir. 40 (3) (2013) 221–226.
[45] D. Kahn, et al., Partial hepatectomy and liver regeneration in pigs–the response to different resection sizes, J. Surg. Res. 45 (2) (1988) 176–180.
[46] F.A. Osman, et al., Gross anatomical studies on the portal vein, hepatic artery and bile duct in the liver of the pig, Journal of Veterinary Anatomy 1 (1) (2008) 59–72.
[47] A. Ntonas, et al., Comparative anatomical study between the human and swine liver and its importance in xenotransplantation, Cureus 12 (7) (2020) e9411.
[48] B.V. Ülger, et al., Variations in the vascular and biliary structures of the liver: a comprehensive anatomical study, Acta Chir. Belg. 118 (6) (2018) 354–371.
[49] J.E. Skandalakis, et al., Hepatic surgical anatomy, Surg. Clin. 84 (2) (2004), 413-35, viii.
[50] I.V. Kholodenko, K.N. Yarygin, Cellular mechanisms of liver regeneration and cell-based therapies of liver diseases, BioMed Res. Int. 2017 (2017) 8910821.
[51] C. Tian, et al., A hepatoprotective role of peritumoral non-parenchymal cells in early liver tumorigenesis, Dis. Model. Mech. 16 (3) (2023).
[52] K.M. Mak, D.W. Shin, Hepatic sinusoids versus central veins: structures, markers, angiocrines, and roles in liver regeneration and homeostasis, Anat. Rec. 304 (8) (2021) 1661–1691.
[53] K. Kamimura, et al., Image-guided, lobe-specific hydrodynamic gene delivery to swine liver, Mol. Ther. 17 (3) (2009) 491–499.
[54] S.-J. Estermann, et al., Comparison of Thiel preserved, fresh human, and animal liver tissue in terms of mechanical properties, Ann. Anatom. - Anatomischer. Anzeiger 236 (2021) 151717.
[55] A.R. Kemper, et al., Biomechanical response of human liver in tensile loading, Ann. Adv. Automot. Med. 54 (2010) 15–26.
[56] A.A. Golebiowska, et al., Decellularized extracellular matrix biomaterials for regenerative therapies: advances, challenges and clinical prospects, Bioact. Mater. 32 (2024) 98–123.
[57] V. Agrawal, et al., Recruitment of progenitor cells by an extracellular matrix cryptic peptide in a mouse model of digit amputation, Tissue Eng. 17 (19–20) (2011) 2435–2443.
[58] M.T. Wolf, et al., Biologic scaffold composed of skeletal muscle extracellular matrix, Biomaterials 33 (10) (2012) 2916–2925.
[59] T.W. Gilbert, T.L. Sellaro, S.F. Badylak, Decellularization of tissues and organs, Biomaterials 27 (19) (2006) 3675–3683.
[60] M.H. Zheng, et al., Porcine small intestine submucosa (SIS) is not an acellular collagenous matrix and contains porcine DNA: possible implications in human implantation, J. Biomed. Mater. Res. B Appl. Biomater. 73 (1) (2005) 61–67.
[61] P. Simon, et al., Early failure of the tissue engineered porcine heart valve SYNERGRAFT in pediatric patients, Eur. J. Cardio. Thorac. Surg. 23 (6) (2003) 1002–1006. ; discussion 1006.
[62] Y. Wang, et al., Recent advances in decellularization and recellularization for tissue-engineered liver grafts, Cells Tissues Organs 204 (3–4) (2017) 125–136.
[63] R.D. Record Ritchie, et al., Lack of immunogenicity of xenogeneic DNA from porcine biomaterials, Surg. Open Sci. 10 (2022) 83–90.
[64] U. Galili, The α-Gal epitope (Galα1-3Galβ1-4GlcNAc-R) in xenotransplantation, Biochimie 83 (7) (2001) 557–563.
[65] U. Galili, Anti-Gal: an abundant human natural antibody of multiple pathogeneses and clinical benefits, Immunology 140 (1) (2013) 1–11.
[66] U. Galili, K. Swanson, Gene sequences suggest inactivation of alpha-1,3-galactosyltransferase in catarrhines after the divergence of apes from monkeys, Proc. Natl. Acad. Sci. U. S. A. 88 (16) (1991) 7401–7404.
[67] K.H. Hussein, et al., Construction of a biocompatible decellularized porcine hepatic lobe for liver bioengineering, Int. J. Artif. Organs 38 (2) (2015) 96–104.
[68] K.-M. Park, et al., Preparation of immunogen-reduced and biocompatible extracellular matrices from porcine liver, J. Biosci. Bioeng. 115 (2) (2013) 207–215.
[69] Y. Wang, et al., Genipin crosslinking reduced the immunogenicity of xenogeneic decellularized porcine whole-liver matrices through regulation of immune cell proliferation and polarization, Sci. Rep. 6 (2016) 24779.
[70] R. Amon, et al., Glycans in immune recognition and response, Carbohydr. Res. 389 (2014) 115–122.
[71] A. Zhu, R. Hurst, Anti-N-glycolylneuraminic acid antibodies identified in healthy human serum, Xenotransplantation 9 (6) (2002) 376–381.
[72] A.J. Tector, et al., The possible role of anti-Neu5Gc as an obstacle in xenotransplantation, Front. Immunol. 11 (2020).
[73] C.E. McQuitty, et al., Immunomodulatory role of the extracellular matrix within the liver disease microenvironment, Front. Immunol. 11 (2020) 574276.
[74] A.T. Rowley, et al., Extracellular matrix-based strategies for immunomodulatory biomaterials engineering, Adv. Healthcare Mater. 8 (8) (2019) 1801578.
[75] T.L. Adair-Kirk, et al., A chemotactic peptide from laminin alpha 5 functions as a regulator of inflammatory immune responses via TNF alpha-mediated signaling, J. Immunol. 174 (3) (2005) 1621–1629.
[76] M. Lopera Higuita, L.G. Griffiths, Antigen removal process preserves function of small diameter venous valved conduits, whereas SDS-decellularization results in significant valvular insufficiency, Acta Biomater. 107 (2020) 115–128.
[77] J. Holl, et al., Skin substitute preparation method induces immunomodulatory changes in Co-incubated cells through collagen modification, Pharmaceutics 13 (12) (2021) 2164.
[78] S. Mehraban, et al., The proinflammatory activity of structurally altered elastic fibers, Am. J. Respir. Cell Mol. Biol. 63 (5) (2020) 699–706.
[79] J.-S. Zhou, et al., Cigarette smoke-initiated autoimmunity facilitates sensitisation to elastin-induced COPD-like pathologies in mice, Eur. Respir. J. 56 (3) (2020) 2000404.
[80] M. Kasravi, et al., Immunogenicity of decellularized extracellular matrix scaffolds: a bottleneck in tissue engineering and regenerative medicine, Biomater. Res. 27 (1) (2023) 10.
[81] A. Bayrak, et al., Human immune responses to porcine xenogeneic matrices and their extracellular matrix constituents in vitro, Biomaterials 31 (14) (2010) 3793–3803.
[82] S.T. LoPresti, B.N. Brown, Effect of source animal age upon macrophage response to extracellular matrix biomaterials, J. Immunol. Regener. Med. 1 (2018) 57–66.
[83] R.M. Wang, et al., Humanized mouse model for assessing the human immune response to xenogeneic and allogeneic decellularized biomaterials, Biomaterials 129 (2017) 98–110.
[84] Z. Wang, et al., Decellularized neonatal cardiac extracellular matrix prevents widespread ventricular remodeling in adult mammals after myocardial infarction, Acta Biomater. 87 (2019) 140–151.
[85] L.M. Godin, et al., Decreased laminin expression by human lung epithelial cells and fibroblasts cultured in acellular lung scaffolds from aged mice, PLoS One 11 (3) (2016) e0150966.
[86] J.S. Lwebuga-Mukasa, D.H. Ingbar, J.A. Madri, Repopulation of a human alveolar matrix by adult rat type II pneumocytes in vitro: a novel system for type II pneumocyte culture, Exp. Cell Res. 162 (2) (1986) 423–435.
[87] E. Meezan, et al., A simple, versatile, nondisruptive method for the isolation of morphologically and chemically pure basement membranes from several tissues, Life Sci. 17 (11) (1975) 1721–1732.
[88] M. Rojkind, et al., Connective tissue biomatrix: its isolation and utilization for long-term cultures of normal rat hepatocytes, J. Cell Biol. 87 (1) (1980) 255–263.
[89] H.C. Ott, et al., Perfusion-decellularized matrix: using nature's platform to engineer a bioartificial heart, Nat. Med. 14 (2) (2008) 213–221.
[90] D.C. Sullivan, et al., Decellularization methods of porcine kidneys for whole organ engineering using a high-throughput system, Biomaterials 33 (31) (2012) 7756–7764.
[91] J.J. Song, et al., Regeneration and experimental orthotopic transplantation of a bioengineered kidney, Nat. Med. 19 (5) (2013) 646–651.
[92] E.E. Friedrich, et al., Residual sodium dodecyl sulfate in decellularized muscle matrices leads to fibroblast activation in vitro and foreign body response in vivo, J. Tissue Eng. Regener. Med. 12 (3) (2018) e1704–e1715.
[93] L.J. White, et al., The impact of detergents on the tissue decellularization process: a ToF-SIMS study, Acta Biomater. 50 (2017) 207–219.
[94] M.J. Sawkins, et al., Hydrogels derived from demineralized and decellularized bone extracellular matrix, Acta Biomater. 9 (8) (2013) 7865–7873.

[95] Y. Wang, et al., Method for perfusion decellularization of porcine whole liver and kidney for use as a scaffold for clinical-scale bioengineering engrafts, Xenotransplantation 22 (1) (2015) 48–61.
[96] D. Koley, A.J. Bard, Triton X-100 concentration effects on membrane permeability of a single HeLa cell by scanning electrochemical microscopy (SECM), Proc. Natl. Acad. Sci. USA 107 (39) (2010) 16783–16787.
[97] J. Welch, et al., Evaluation of the toxicity of sodium dodecyl sulphate (SDS) in the MucilAir™ human airway model in vitro, Regul. Toxicol. Pharmacol. 125 (2021) 105022.
[98] J. Fernández-Pérez, M. Ahearne, The impact of decellularization methods on extracellular matrix derived hydrogels, Sci. Rep. 9 (1) (2019) 14933.
[99] T.J. Keane, I.T. Swinehart, S.F. Badylak, Methods of tissue decellularization used for preparation of biologic scaffolds and in vivo relevance, Methods 84 (2015) 25–34.
[100] S.P. Wilshaw, et al., Biocompatibility and potential of acellular human amniotic membrane to support the attachment and proliferation of allogeneic cells, Tissue Eng. 14 (4) (2008) 463–472.
[101] H. Ren, et al., Evaluation of two decellularization methods in the development of a whole-organ decellularized rat liver scaffold, Liver Int. 33 (3) (2013) 448–458.
[102] N. Poornejad, et al., The impact of decellularization agents on renal tissue extracellular matrix, J. Biomater. Appl. 31 (4) (2016) 521–533.
[103] L. Moradi, et al., Evaluation of different sterilization methods for decellularized kidney tissue, Tissue Cell 66 (2020) 101396.
[104] K.H. Hussein, et al., Sterilization using electrolyzed water highly retains the biological properties in tissue-engineered porcine liver scaffold, Int. J. Artif. Organs 36 (11) (2013) 781–792.
[105] P. Zhou, et al., Decellularization and recellularization of rat livers with hepatocytes and endothelial progenitor cells, Artif. Organs 40 (3) (2016) E25–E38.
[106] O. Syed, et al., Evaluation of decellularization protocols for production of tubular small intestine submucosa scaffolds for use in oesophageal tissue engineering, Acta Biomater. 10 (12) (2014) 5043–5054.
[107] S.K. Gupta, N.C. Mishra, A. Dhasmana, Decellularization methods for scaffold fabrication, Methods Mol. Biol. 1577 (2018) 1–10.
[108] F. Meng, et al., Vasculature reconstruction of decellularized liver scaffolds via gelatin-based re-endothelialization, J. Biomed. Mater. Res. 107 (2) (2019) 392–402.
[109] T. Tsuchiya, et al., Influence of pH on extracellular matrix preservation during lung decellularization, Tissue Eng. C Methods 20 (12) (2014) 1028–1036.
[110] A. Soto-Gutierrez, et al., A whole-organ regenerative medicine approach for liver replacement, Tissue Eng. C Methods 17 (6) (2011) 677–686.
[111] Y. Chen, et al., Repopulation of intrahepatic bile ducts in engineered rat liver grafts, Technology 7 (1–2) (2019) 46–55.
[112] O. Gorschewsky, et al., Clinical comparison of the tutoplast allograft and autologous patellar tendon (Bone-Patellar tendon-bone) for the reconstruction of the anterior cruciate ligament: 2- and 6-year results, Am. J. Sports Med. 33 (8) (2005) 1202–1209.
[113] M.C. Jamur, C. Oliver, Cell fixatives for immunostaining, in: C. Oliver, M. C. Jamur (Eds.), Immunocytochemical Methods and Protocols, Humana Press, Totowa, NJ, 2010, pp. 55–61.
[114] H. Wang, W.Q. Sun, J. Wang, Complete proteomic profiling of regenerative bio-scaffolds with a two-step trypsinization method, J. Biomed. Mater. Res. B Appl. Biomater. 111 (1) (2023) 62–72.
[115] B. Cox, A. Emili, Tissue subcellular fractionation and protein extraction for use in mass-spectrometry-based proteomics, Nat. Protoc. 1 (4) (2006) 1872–1878.
[116] C.C. Xu, R.W. Chan, N. Tirunagari, A biodegradable, acellular xenogeneic scaffold for regeneration of the vocal fold lamina propria, Tissue Eng. 13 (3) (2007) 551–566.
[117] S.L. Dahl, et al., Decellularized native and engineered arterial scaffolds for transplantation, Cell Transplant. 12 (6) (2003) 659–666.
[118] P.A. Aeberhard, et al., Efficient decellularization of equine tendon with preserved biomechanical properties and cytocompatibility for human tendon surgery indications, Artif. Organs 44 (4) (2020) E161–e171.
[119] J.K. Kim, et al., Development of a decellularization method to produce nerve allografts using less invasive detergents and hyper/hypotonic solutions, J. Plast. Reconstr. Aesthetic Surg. 69 (12) (2016) 1690–1696.
[120] R.C. Cornelison, et al., Development of an apoptosis-assisted decellularization method for maximal preservation of nerve tissue structure, Acta Biomater. 77 (2018) 116–126.
[121] J.E. Kobes, et al., A comparison of iron oxide particles and silica particles for tracking organ recellularization, Mol. Imag. 17 (2018) 1536012118787322.
[122] S.P. Roth, et al., Automated freeze-thaw cycles for decellularization of tendon tissue - a pilot study, BMC Biotechnol. 17 (1) (2017) 13.
[123] Y. Kadota, et al., Mesenchymal stem cells support hepatocyte function in engineered liver grafts, Organogenesis 10 (2) (2014) 268–277.
[124] X. Liu, et al., An innovative method to obtain porous porcine aorta scaffolds for tissue engineering, Artif. Organs 43 (12) (2019) 1162–1169.
[125] A. Hopkinson, et al., Optimization of amniotic membrane (AM) denuding for tissue engineering, Tissue Eng. C Methods 14 (4) (2008) 371–381.
[126] I. Prasertsung, et al., Development of acellular dermis from porcine skin using periodic pressurized technique, J. Biomed. Mater. Res. B Appl. Biomater. 85B (1) (2008) 210–219.
[127] C.D. Plant, G.W. Plant, Viral transduction of schwann cells for peripheral nerve repair, Methods Mol. Biol. 1739 (2018) 455–466.
[128] J. Burk, et al., Freeze-thaw cycles enhance decellularization of large tendons, Tissue Eng. C Methods 20 (4) (2014) 276–284.
[129] J. Cheng, C. Wang, Y. Gu, Combination of freeze-thaw with detergents: a promising approach to the decellularization of porcine carotid arteries, Bio Med. Mater. Eng. 30 (2) (2019) 191–205.
[130] Pulver, et al., Production of organ extracellular matrix using a freeze-thaw cycle employing extracellular cryoprotectants, Cryo Lett. 35 (5) (2014) 400–406.
[131] M. Ashokkumar, The characterization of acoustic cavitation bubbles - an overview, Ultrason. Sonochem. 18 (4) (2011) 864–872.
[132] F. Forouzesh, M. Rabbani, S. Bonakdar, A comparison between ultrasonic bath and direct sonicator on osteochondral tissue decellularization, J Med Signals Sens 9 (4) (2019) 227–233.
[133] F. Yusof, M. Sha'ban, A. Azhim, Development of decellularized meniscus using closed sonication treatment system: potential scaffolds for orthopedics tissue engineering applications, Int. J. Nanomed. 14 (2019) 5491–5502.
[134] C.H. Lin, et al., Sonication-Assisted method for decellularization of human umbilical artery for small-caliber vascular tissue engineering, Polymers 13 (11) (2021).
[135] W. Shen, et al., Rapid and detergent-free decellularization of cartilage, Tissue Eng. C Methods 26 (4) (2020) 201–206.
[136] S.H. Hung, et al., Larynx decellularization: combining freeze-drying and sonication as an effective method, J. Voice 27 (3) (2013) 289–294.
[137] G. Almeida, et al., Perfusion and ultrasonication produce a decellularized porcine whole-ovary scaffold with a preserved microarchitecture, Cells 12 (14) (2023).
[138] T.M. Manalastas, et al., Effect of decellularization parameters on the efficient production of kidney bioscaffolds, Appl. Biochem. Biotechnol. 193 (5) (2021) 1239–1251.
[139] M.B. Sano, et al., Towards the creation of decellularized organ constructs using irreversible electroporation and active mechanical perfusion, Biomed. Eng. Online 9 (2010) 83.
[140] A. Golberg, et al., Rat liver regeneration following ablation with irreversible electroporation, PeerJ 4 (2016) e1571.
[141] A. Saini, et al., Irreversible electroporation in liver cancers and whole organ engineering, J. Clin. Med. 8 (1) (2018).
[142] T.T. Chang, V.X. Zhou, B. Rubinsky, Using non-thermal irreversible electroporation to create an in vivo niche for exogenous cell engraftment, Biotechniques 62 (5) (2017) 229–231.
[143] Y. Zager, et al., Optimization of irreversible electroporation protocols for in-vivo myocardial decellularization, PLoS One 11 (11) (2016) e0165475.
[144] M. Phillips, E. Maor, B. Rubinsky, Nonthermal irreversible electroporation for tissue decellularization, J. Biomech. Eng. 132 (9) (2010) 091003.
[145] Y. Zhang, et al., Molecular and histological study on the effects of non-thermal irreversible electroporation on the liver, Biochem. Biophys. Res. Commun. 500 (3) (2018) 665–670.
[146] Q. Dai, et al., Recent advances in liver engineering with decellularized scaffold, Front. Bioeng. Biotechnol. 10 (2022) 831477.
[147] L. Gui, et al., Novel utilization of serum in tissue decellularization, Tissue Eng. C Methods 16 (2) (2010) 173–184.
[148] J.Y. Oh, et al., Processing porcine cornea for biomedical applications, Tissue Eng. C Methods 15 (4) (2009) 635–645.
[149] N.E.M. Bühler, et al., Controlled processing of a full-sized porcine liver to a decellularized matrix in 24 h, J. Biosci. Bioeng. 119 (5) (2015) 609–613.
[150] M. Watanabe, et al., Construction of sinusoid-scale microvessels in perfusion culture of a decellularized liver, Acta Biomater. 95 (2019) 307–318.
[151] W. Yang, Nucleases: diversity of structure, function and mechanism, Q. Rev. Biophys. 44 (1) (2011) 1–93.
[152] S.L. Wilson, et al., Corneal decellularization: a method of recycling unsuitable donor tissue for clinical translation? Curr. Eye Res. 41 (6) (2016) 769–782.
[153] M.W. McCrary, et al., Novel sodium deoxycholate-based chemical decellularization method for peripheral nerve, Tissue Eng. C Methods 26 (1) (2020) 23–36.
[154] M. Su, et al., Preparation of decellularized triphasic hierarchical bone-fibrocartilage-tendon composite extracellular matrix for enthesis regeneration, Adv. Healthcare Mater. 8 (19) (2019) e1900831.
[155] G.H. Yam, et al., Decellularization of human stromal refractive lenticules for corneal tissue engineering, Sci. Rep. 6 (2016) 26339.
[156] J.A. Mótyán, F. Tóth, J. Tőzsér, Research applications of proteolytic enzymes in molecular biology, Biomolecules 3 (4) (2013) 923–942.
[157] X. Zhang, et al., Decellularized extracellular matrix scaffolds: recent trends and emerging strategies in tissue engineering, Bioact. Mater. 10 (2022) 15–31.
[158] K. Schenke-Layland, et al., Impact of decellularization of xenogeneic tissue on extracellular matrix integrity for tissue engineering of heart valves, J. Struct. Biol. 143 (3) (2003) 201–208.
[159] R.W. Grauss, et al., Histological evaluation of decellularised porcine aortic valves: matrix changes due to different decellularisation methods☆, Eur. J. Cardio. Thorac. Surg. 27 (4) (2005) 566–571.
[160] J. Paulo Zambon, A. Atala, J.J. Yoo, Methods to generate tissue-derived constructs for regenerative medicine applications, Methods 171 (2020) 3–10.
[161] C.H. Lin, et al., An investigation on the correlation between the mechanical property change and the alterations in composition and microstructure of a porcine vascular tissue underwent trypsin-based decellularization treatment, J. Mech. Behav. Biomed. Mater. 86 (2018) 199–207.
[162] R.C. Gessner, et al., Functional ultrasound imaging for assessment of extracellular matrix scaffolds used for liver organoid formation, Biomaterials 34 (37) (2013) 9341–9351.
[163] M. Marzaro, et al., Decellularized esophageal tubular scaffold microperforated by quantum molecular resonance technology and seeded with mesenchymal stromal

cells for tissue engineering esophageal regeneration, Front. Bioeng. Biotechnol. 10 (2022).
[164] S. Barbon, et al., Bio-engineered scaffolds derived from decellularized human esophagus for functional organ reconstruction, Cells 11 (19) (2022).
[165] C.-Y. Kao, H.-Q.-D. Nguyen, Y.-C. Weng, Characterization of porcine urinary bladder matrix hydrogels from sodium dodecyl sulfate decellularization method, Polymers 12 (12) (2020) 3007.
[166] P. Giuffrida, et al., Decellularized human gut as a natural 3D platform for research in intestinal fibrosis, Inflamm. Bowel Dis. 25 (11) (2019) 1740–1750.
[167] Z.H. Tan, et al., Regeneration of tracheal neotissue in partially decellularized scaffolds, npj Regener. Med. 8 (1) (2023) 35.
[168] K.H. Hussein, et al., Vascular reconstruction: a major challenge in developing a functional whole solid organ graft from decellularized organs, Acta Biomater. 103 (2020) 68–80.
[169] D. Seetapun, J.J. Ross, Eliminating the organ transplant waiting list: the future with perfusion decellularized organs, Surgery 161 (6) (2017) 1474–1478.
[170] B. Struecker, et al., Improved rat liver decellularization by arterial perfusion under oscillating pressure conditions, J. Tissue Eng. Regen. Med. 11 (2) (2017) 531–541.
[171] C.R. Rowland, et al., The effects of crosslinking of scaffolds engineered from cartilage ECM on the chondrogenic differentiation of MSCs, Biomaterials 34 (23) (2013) 5802–5812.
[172] B. Ma, et al., Crosslinking strategies for preparation of extracellular matrix-derived cardiovascular scaffolds, Regen. Biomater. 1 (1) (2014) 81–89.
[173] K.H. Hussein, et al., New insights into the pros and cons of cross-linking decellularized bioartificial organs, Int. J. Artif. Organs 40 (4) (2017) 136–141.
[174] D.W. Courtman, B.F. Errett, G.J. Wilson, The role of crosslinking in modification of the immune response elicited against xenogenic vascular acellular matrices, J. Biomed. Mater. Res. 55 (4) (2001) 576–586.
[175] X. Wang, et al., Procyanidins-crosslinked aortic elastin scaffolds with distinctive anti-calcification and biological properties, Acta Biomater. 16 (2015) 81–93.
[176] C.E. Schmidt, J.M. Baier, Acellular vascular tissues: natural biomaterials for tissue repair and tissue engineering, Biomaterials 21 (22) (2000) 2215–2231.
[177] T. Saleh, et al., Silver nanoparticles improve structural stability and biocompatibility of decellularized porcine liver, Artif. Cells, Nanomed. Biotechnol. 46 (sup2) (2018) 273–284.
[178] D.-H. Kim, et al., Bioengineered liver crosslinked with nano-graphene oxide enables efficient liver regeneration via MMP suppression and immunomodulation, Nat. Commun. 14 (1) (2023) 801.
[179] M. Tao, et al., Sterilization and disinfection methods for decellularized matrix materials: review, consideration and proposal, Bioact. Mater. 6 (9) (2021) 2927–2945.
[180] T. Goecke, et al., In vivo performance of freeze-dried decellularized pulmonary heart valve allo- and xenografts orthotopically implanted into juvenile sheep, Acta Biomater. 68 (2018) 41–52.
[181] S. Qiu, et al., Decellularized nerve matrix hydrogel and glial-derived neurotrophic factor modifications assisted nerve repair with decellularized nerve matrix scaffolds, J. Tissue Eng. Regen. Med. 14 (7) (2020) 931–943.
[182] W.Q. Sun, P. Leung, Calorimetric study of extracellular tissue matrix degradation and instability after gamma irradiation, Acta Biomater. 4 (4) (2008) 817–826.
[183] S.-H. Mirmalek-Sani, et al., Immunogenicity of decellularized porcine liver for bioengineered hepatic tissue, Am. J. Pathol. 183 (2) (2013) 558–565.
[184] G. Mattei, et al., Mechanostructure and composition of highly reproducible decellularized liver matrices, Acta Biomater. 10 (2) (2014) 875–882.
[185] S. Cebotari, et al., Detergent decellularization of heart valves for tissue engineering: toxicological effects of residual detergents on human endothelial cells, Artif. Organs 34 (3) (2010) 206–210.
[186] A.J. Dalgliesh, et al., Graft-specific immune tolerance is determined by residual antigenicity of xenogeneic extracellular matrix scaffolds, Acta Biomater. 79 (2018) 253–264.
[187] M. Arand, T. Friedberg, F. Oesch, Colorimetric quantitation of trace amounts of sodium lauryl sulfate in the presence of nucleic acids and proteins, Anal. Biochem. 207 (1) (1992) 73–75.
[188] F. Rusconi, et al., Quantification of sodium dodecyl sulfate in microliter-volume biochemical samples by visible light spectroscopy, Anal. Biochem. 295 (1) (2001) 31–37.
[189] M. Gordillo, T. Evans, V. Gouon-Evans, Orchestrating liver development, Development 142 (12) (2015) 2094–2108.
[190] N.L. Sussman, J.H. Kelly, Artificial liver: a forthcoming attraction, Hepatology 17 (6) (1993) 1163–1164.
[191] R. Manco, I.A. Leclercq, L.A. Clerbaux, Liver regeneration: different sub-populations of parenchymal cells at play choreographed by an injury-specific microenvironment, Int. J. Mol. Sci. 19 (12) (2018).
[192] B. Toprakhisar, C.M. Verfaillie, M. Kumar, Advances in recellularization of decellularized liver grafts with different liver (stem) cells: towards clinical applications, Cells 12 (2) (2023).
[193] B.D. Anderson, et al., Functional characterization of a bioengineered liver after heterotopic implantation in pigs, Commun. Biol. 4 (1) (2021) 1157.
[194] W. Hassanein, et al., Recellularization via the bile duct supports functional allogenic and xenogenic cell growth on a decellularized rat liver scaffold, Organogenesis 13 (1) (2017) 16–27.
[195] H. Kojima, et al., Establishment of practical recellularized liver graft for blood perfusion using primary rat hepatocytes and liver sinusoidal endothelial cells, Am. J. Transplant. 18 (6) (2018) 1351–1359.
[196] D.M. Faulk, J.D. Wildemann, S.F. Badylak, Decellularization and cell seeding of whole liver biologic scaffolds composed of extracellular matrix, J. Clin. Exp. Hepatol. 5 (1) (2015) 69–80.
[197] A.A. Palakkan, et al., Liver tissue engineering and cell sources: issues and challenges, Liver Int. 33 (5) (2013) 666–676.
[198] H. Yagi, et al., Human-scale whole-organ bioengineering for liver transplantation: a regenerative medicine approach, Cell Transplant. 22 (2) (2013) 231–242.
[199] S.L. Nyberg, et al., Demonstration of biochemical function by extracorporeal xenohepatocytes in an anhepatic animal model, Transplant. Proc. 25 (2) (1993) 1944–1945.
[200] V. Dixit, G. Gitnick, Artificial liver support: state of the art, Scand. J. Gastroenterol. Suppl. 220 (1996) 101–114.
[201] Q. Yang, et al., Fluidized-bed bioartificial liver assist devices (BLADs) based on microencapsulated primary porcine hepatocytes have risk of porcine endogenous retroviruses transmission, Hepatol. Int. 4 (4) (2010) 757–761.
[202] A. Kumar, A. Tripathi, S. Jain, Extracorporeal bioartificial liver for treating acute liver diseases, J. Extra Corpor. Technol. 43 (4) (2011) 195–206.
[203] T. Debnath, C.S. Mallarpu, L.K. Chelluri, Development of bioengineered organ using biological acellular rat liver scaffold and hepatocytes, Organogenesis 16 (2) (2020) 61–72.
[204] K.H. Hussein, et al., Three dimensional culture of HepG2 liver cells on a rat decellularized liver matrix for pharmacological studies, J. Biomed. Mater. Res. B Appl. Biomater. 104 (2) (2016) 263–273.
[205] S.L. Nyberg, et al., Primary hepatocytes outperform Hep G2 cells as the source of biotransformation functions in a bioartificial liver, Ann. Surg. 220 (1) (1994) 59–67.
[206] A. Ring, et al., Hepatic maturation of human fetal hepatocytes in four-compartment three-dimensional perfusion culture, Tissue Eng. C Methods 16 (5) (2010) 835–845.
[207] P.P. Poyck, et al., Functional and morphological comparison of three primary liver cell types cultured in the AMC bioartificial liver, Liver Transplant. 13 (4) (2007) 589–598.
[208] S. Diekmann, A. Bader, S. Schmitmeier, Present and Future Developments in Hepatic Tissue Engineering for Liver Support Systems : state of the art and future developments of hepatic cell culture techniques for the use in liver support systems, Cytotechnology 50 (1–3) (2006) 163–179.
[209] T. Tricot, J. De Boeck, C. Verfaillie, Alternative cell sources for liver parenchyma repopulation: where do we stand? Cells 9 (3) (2020).
[210] S.H. Kang, et al., Mesenchymal stem cells for the treatment of liver disease: present and perspectives, Gut Liver 14 (3) (2020) 306–315.
[211] W.-C. Jiang, et al., Cryo-chemical decellularization of the whole liver for mesenchymal stem cells-based functional hepatic tissue engineering, Biomaterials 35 (11) (2014) 3607–3617.
[212] K. Takahashi, S. Yamanaka, Induction of pluripotent stem cells from mouse embryonic and adult fibroblast cultures by defined factors, Cell 126 (4) (2006) 663–676.
[213] K.M. Park, et al., Decellularized liver extracellular matrix as promising tools for transplantable bioengineered liver promotes hepatic lineage commitments of induced pluripotent stem cells, Tissue Eng. 22 (5–6) (2016) 449–460.
[214] T. Minami, et al., Novel hybrid three-dimensional artificial liver using human induced pluripotent stem cells and a rat decellularized liver scaffold, Regener. Ther. 10 (2019) 127–133.
[215] A. Acun, et al., Human-origin iPSC-based recellularization of decellularized whole rat livers, Bioengineering 9 (5) (2022).
[216] U. Ben-David, N. Benvenisty, The tumorigenicity of human embryonic and induced pluripotent stem cells, Nat. Rev. Cancer 11 (4) (2011) 268–277.
[217] S. Ogiso, et al., Efficient recellularisation of decellularised whole-liver grafts using biliary tree and foetal hepatocytes, Sci. Rep. 6 (1) (2016) 35887.
[218] J. Bao, et al., Construction of a portal implantable functional tissue-engineered liver using perfusion-decellularized matrix and hepatocytes in rats, Cell Transplant. 20 (5) (2011) 753–766.
[219] J. Bao, et al., Hemocompatibility improvement of perfusion-decellularized clinical-scale liver scaffold through heparin immobilization, Sci. Rep. 5 (1) (2015) 10756.
[220] G. Orlando, et al., Production and implantation of renal extracellular matrix scaffolds from porcine kidneys as a platform for renal bioengineering investigations, Ann. Surg. 256 (2) (2012) 363–370.
[221] M.T. Kasimir, et al., Decellularization does not eliminate thrombogenicity and inflammatory stimulation in tissue-engineered porcine heart valves, J. Heart Valve Dis. 15 (2) (2006) 278–286. ; discussion 286.
[222] K. Li, et al., Re-endothelialization of decellularized liver scaffolds: a step for bioengineered liver transplantation, Front. Bioeng. Biotechnol. 10 (2022) 833163.
[223] J. Folkman, M. Hochberg, Self-regulation of growth in three dimensions, J. Exp. Med. 138 (4) (1973) 745–753.
[224] Y. Nahmias, et al., A novel formulation of oxygen-carrying matrix enhances liver-specific function of cultured hepatocytes, Faseb. J. 20 (14) (2006) 2531–2533.
[225] S. Bae, et al., Heparin-eluting electrospun nanofiber yarns for antithrombotic vascular sutures, ACS Appl. Mater. Interfaces 10 (10) (2018) 8426–8435.
[226] X. Ye, et al., The effect of heparin-VEGF multilayer on the biocompatibility of decellularized aortic valve with platelet and endothelial progenitor cells, PLoS One 8 (1) (2013) e54622.
[227] H. Hajiali, et al., Electrospun PGA/gelatin nanofibrous scaffolds and their potential application in vascular tissue engineering, Int. J. Nanomed. 6 (2011) 2133–2141.

[228] B. Dhandayuthapani, U.M. Krishnan, S. Sethuraman, Fabrication and characterization of chitosan-gelatin blend nanofibers for skin tissue engineering, J. Biomed. Mater. Res. B Appl. Biomater. 94B (1) (2010) 264–272.
[229] S.P. Massia, J.A. Hubbell, Vascular endothelial cell adhesion and spreading promoted by the peptide REDV of the IIICS region of plasma fibronectin is mediated by integrin alpha 4 beta 1, J. Biol. Chem. 267 (20) (1992) 14019–14026.
[230] M.J. Humphries, et al., Identification of an alternatively spliced site in human plasma fibronectin that mediates cell type-specific adhesion, J. Cell Biol. 103 (6 Pt 2) (1986) 2637–2647.
[231] T.M. Bedair, et al., Recent advances to accelerate re-endothelialization for vascular stents, J. Tissue Eng. 8 (2017) 2041731417731546.
[232] H. Chen, et al., Biocompatible polymer materials: role of protein–surface interactions, Prog. Polym. Sci. 33 (11) (2008) 1059–1087.
[233] B.A. Butruk-Raszeja, et al., Endothelialization of polyurethanes: surface silanization and immobilization of REDV peptide, Colloids Surf. B Biointerfaces 144 (2016) 335–343.
[234] I. Adipurnama, et al., Surface modification and endothelialization of polyurethane for vascular tissue engineering applications: a review, Biomater. Sci. 5 (1) (2017) 22–37.
[235] B.M. Bourke, W.R. Roche, M. Appleberg, Endothelial cell harvest for seeding vascular prostheses: the influence of technique on cell function, viability, and number, J. Vasc. Surg. 4 (3) (1986) 257–263.
[236] H.H.G. Song, et al., Vascular tissue engineering: progress, challenges, and clinical promise, Cell Stem Cell 22 (3) (2018) 340–354.
[237] N. Koike, et al., Creation of long-lasting blood vessels, Nature 428 (6979) (2004) 138–139.
[238] V.V. Orlova, et al., Generation, expansion and functional analysis of endothelial cells and pericytes derived from human pluripotent stem cells, Nat. Protoc. 9 (6) (2014) 1514–1531.
[239] R.P. Visconti, et al., Towards organ printing: engineering an intra-organ branched vascular tree, Expet Opin. Biol. Ther. 10 (3) (2010) 409–420.
[240] Z. Wang, et al., Rapid vascularization of tissue-engineered vascular grafts in vivo by endothelial cells in co-culture with smooth muscle cells, J. Mater. Sci. Mater. Med. 23 (4) (2012) 1109–1117.
[241] C.R. Balistreri, et al., Are endothelial progenitor cells the real solution for cardiovascular diseases? Focus on controversies and perspectives, BioMed Res. Int. 2015 (2015) 835934.
[242] K. Takeishi, et al., Assembly and function of a bioengineered human liver for transplantation generated solely from induced pluripotent stem cells, Cell Rep. 31 (9) (2020) 107711.
[243] J.L. Boyer, Bile formation and secretion, Compr. Physiol. 3 (3) (2013) 1035–1078.
[244] J.M. Banales, et al., Cholangiocyte pathobiology, Nat. Rev. Gastroenterol. Hepatol. 16 (5) (2019) 269–281.
[245] E. Mazari-Arrighi, et al., Construction of functional biliary epithelial branched networks with predefined geometry using digital light stereolithography, Biomaterials 279 (2021) 121207.
[246] R. Joplin, Isolation and culture of biliary epithelial cells, Gut 35 (7) (1994) 875–878.
[247] R. Kudira, et al., Isolation and culturing primary chaolangiocytes from mouse liver, Bio Protoc. 11 (20) (2021) e4192.
[248] A. Marsee, et al., Building consensus on definition and nomenclature of hepatic, pancreatic, and biliary organoids, Cell Stem Cell 28 (5) (2021) 816–832.
[249] F.J.M. Roos, et al., Cholangiocyte organoids from human bile retain a local phenotype and can repopulate bile ducts in vitro, Clin. Transl. Med. 11 (12) (2021) e566.
[250] M. Huch, et al., Long-term culture of genome-stable bipotent stem cells from adult human liver, Cell 160 (1) (2015) 299–312.
[251] F. Sampaziotis, et al., Reconstruction of the mouse extrahepatic biliary tree using primary human extrahepatic cholangiocyte organoids, Nat. Med. 23 (8) (2017) 954–963.
[252] C.J. Soroka, et al., Bile-derived organoids from patients with primary sclerosing cholangitis recapitulate their inflammatory immune profile, Hepatology 70 (3) (2019) 871–882.
[253] F. Sampaziotis, et al., Cholangiocyte organoids can repair bile ducts after transplantation in the human liver, Science 371 (6531) (2021) 839–846.
[254] C.A. Rimland, et al., Regional differences in human biliary tissues and corresponding in vitro-derived organoids, Hepatology 73 (1) (2021) 247–267.
[255] K. Tomofuji, et al., Liver ductal organoids reconstruct intrahepatic biliary trees in decellularized liver grafts, Biomaterials 287 (2022) 121614.
[256] J. Willemse, et al., Scaffolds obtained from decellularized human extrahepatic bile ducts support organoids to establish functional biliary tissue in a dish, Biotechnol. Bioeng. 118 (2) (2021) 836–851.
[257] T.F. Vandamme, Use of rodents as models of human diseases, J. Pharm. BioAllied Sci. 6 (1) (2014) 2–9.
[258] H. Higashi, et al., Transplantation of bioengineered liver capable of extended function in a preclinical liver failure model, Am. J. Transplant. 22 (3) (2022) 731–744.
[259] FDA Guidance for Industry, Regulation of Human Cells, Tissues, and Cellular and Tissue-Based Products (HCT/Ps) - Small Entity Compliance Guide [cited 2024 February, 2024]; Available from: https://www.fda.gov/regulatory-information/search-fda-guidance-documents/regulation-human-cells-tissues-and-cellular-and-tissue-based-products-hctps-small-entity-compliance, 2022.
[260] A. Barranger, L. Le Hégarat, Towards better prediction of xenobiotic genotoxicity: CometChip technology coupled with a 3D model of HepaRG human liver cells, Arch. Toxicol. 96 (7) (2022) 2087–2095.
[261] L.A. Vernetti, et al., A human liver microphysiology platform for investigating physiology, drug safety, and disease models, Exp. Biol. Med. 241 (1) (2016) 101–114.
[262] A. Skardal, et al., Bioprinting cellularized constructs using a tissue-specific hydrogel bioink, J. Vis. Exp. (110) (2016) e53606.
[263] J.W. Lee, et al., Development of a 3D cell printed construct considering angiogenesis for liver tissue engineering, Biofabrication 8 (1) (2016) 015007.
[264] Clinical trial NCT06285253, A Phase 1 Prospective Study of the Miromatrix External Liver Assist Product (miroliverELAP®) for Liver Support in Adults With Acute Liver Failure [cited 2024 May 27]; Available from: https://classic.clinicaltrials.gov/ct2/show/NCT06285253?id=NCT06285253&draw=2&rank=1&load=cart, 2024.
[265] G.S. Hussey, J.L. Dziki, S.F. Badylak, Extracellular matrix-based materials for regenerative medicine, Nat. Rev. Mater. 3 (7) (2018) 159–173.